Food and Agriculture Organization of the United Nations

UNESCO IHE DELFT

REMOTE SENSING FOR WATER PRODUCTIVITY

WATER ACCOUNTING SERIES

Water Accounting in the Nile River Basin

Water accounting in the Nile River Basin

REMOTE SENSING FOR WATER PRODUCTIVITY

WaPOR water accounting series

Published by
the Food and Agriculture Organization of the United Nations
and
IHE Delft Institute for Water Education

Required citation:

FAO and IHE Delft. 2020. *Water Accounting in the Nile River Basin*. FAO WaPOR water accounting reports. Rome. https://doi.org/10.4060/ca9895en

The designations employed and the presentation of material in this information product do not imply the expression of any opinion whatsoever on the part of the Food and Agriculture Organization of the United Nations (FAO) or –IHE Delft Institute for Water Education (IHE DELFT) concerning the legal or development status of any country, territory, city or area or of its authorities, or concerning the delimitation of its frontiers or boundaries. The mention of specific companies or products of manufacturers, whether or not these have been patented, does not imply that these have been endorsed or recommended by FAO or IHE DELFT in preference to others of a similar nature that are not mentioned. The views expressed in this information product are those of the author(s) and do not necessarily reflect the views or policies of FAO or IHE DELFT. Dashed lines on maps represent approximate border lines for which there may not yet be full agreement.

FAO encourages the use, reproduction and dissemination of material in this information product. Except where otherwise indicated, material may be copied, downloaded and printed for private study, research and teaching purposes, or for use in non-commercial products or services, provided that appropriate acknowledgement of FAO and IHE DELFT as the source and copyright holders is given and that FAO/IHE DELFT's endorsement of users' views, products or services is not implied in any way.

All requests for translation and adaptation rights, and for resale and other commercial use rights should be made via www. fao.org/contact-us/licence-request or addressed to copyright@fao.org.

FAO information products are available on the FAO website (www.fao.org/publications) and can be purchased through publications-sales@fao.org

© FAO and IHE Delft, 2020

978-92-5-132982-5 [FAO]

Cover photo: Blue Nile Falls near Lake Tana, Ethiopia. Photo taken by Solomon Seyoum

Contents

Acronyms and Abbreviations vii

Acknowledgements viii

Executive summary ix

1. Introduction 1

1.1. Case study description 1

1.2. Water resources developments and challenges in Nile River Basin 2

1.3. Objective of Water accounts 3

2. Methodology 5

2.1. WaPOR datasets 5

2.1.1. Precipitation 5

2.1.2. Evapotranspiration 5

2.1.3. Precipitation minus Evapotranspiration 8

2.1.4. Land use analysis 9

2.2. Preliminary assessments 12

2.2.1. Comparison with in situ-observations - Precipitation 12

2.2.2. Comparison of WaPOR ET_a with other ET_a estimates for the Basin 14

2.2.3. Comparison with other remote sensing estimates 16

2.2.4. Conclusion 16

2.3. Other global data sets 17

2.3.1. GRACE 17

2.3.2. Errors in water balance 18

2.3.3. Global maps to categorise land use classes 19

2.4. WA+ methodology 19

2.4.1. Pixel scale analysis 22

2.4.2. Method 22

2.4.3. WaPOR based Water Accounting Plus sheet 1 27

3. Water Accounting Plus 29

3.1. The resource base 29

3.1.1. Overview: Average over the entire period 29

3.1.2. Variability of the annual Water Accounts 30

3.2. Key Indicators 32

3.2.1. ET fraction, Stationarity index and Basin Closure 33

3.2.2. Available water, managed water and managed fraction 33

4. Conclusions 35

References 37

Appendixes 39

Annex 1 Plots of Annual Precipitation of Nile River Basin in mm/year 39

Annex 2 Plots of Annual Actual Evapotranspiration of Nile River Basin in mm/year 41

Annex 3 Plots of Annual P - ET_a of Nile River Basin in mm/year 43

Annex 4 Plots of Annual Land cover classification maps 45

Annex 5 Plots of Annual Land Use maps based on WA+ Categories 47

Annex 6 Annual estimated Incremental ET (ET_{incr}) of individual years 50

Annex 7 Annual estimated Rainfall ET (ET_{rain}) of individual years 52

Annex 8 Annual Water Accounting+ Sheet 1 54

Figures

Figure 1: Location of the Nile River Basin 3

Figure 2: WaPOR annual precipitation (mm/year) for the Nile basin averaged for 2009-18. 6

Figure 3: Annual mean (A) and monthly mean (B) WaPOR Precipitation in Nile River basin for a period of 10 years (2009 to 2018) 6

Figure 4: WaPOR annual actual evapotranspiration and interception (mm/year) for the Nile basin averaged for 2009-2018 7

Figure 5: Annual mean (A) and monthly mean (B) WaPOR Actual Evapotranspiration in Nile River basin for a period of 10 years (2009 to 2018) 7

Figure 6: Precipitation minus Actual Evapotranspiration for the period 2009-2018 8

Figure 7: Land use map of the Awash Basin using WaPOR classification 10

Figure 8: Contribution of the land cover classes to annual precipitation (P) and actual evapotranspiration (ET_a) of the Nile River Basin for the year 2018 10

Figure 9 : Monthly WaPOR precipitation compared with rain gauges in four location in the basin at Debre Markos in Ethiopia, Khartoum in Sudan, Tanta in Egypt and Entebbe in Uganda 13

Figure 10: Comparison of annual ET_a estimates of NBI and WaPOR for major lakes on the Nile River Basin 16

Figure 11: Longer term trend of increasing water storage in Awash Bain on GRACE gravity measurements 17

Figure 12: Error in water balance vs precipitation volume 18

Figure 13: Area percentage of WA+ Land Use categories in Nile River basin in 2018 20

Figure 14: Water accounting flow chart using WaPOR data 21

Figure 15: Main schematization of the flows and fluxes in the WaterPix model 22

Figure 16: Precipitation, ET_{rain} and ET_{incr} per land cover of Nile River Basin for the period 2010 to 2018 26

Figure 17: WA+ sheet 1 for the Awash River Basin containing average flow values for the period 2010 – 2018 30

Figure 18: Nile River Basin water fluxes by year from 2009 to 2018 31

Figure 19: WA+ sheet 1 for the Nile River Basin for the wettest year (2012) 31

Figure 20: WA+ sheet 1 for the Nile River Basin for the driest year (2016) 32

Tables

Table 1: Comparison of annual WaPOR P and ET_a values for the entire Nile Basin 9

Table 2: The mean annual P - ET_a for each land cover class from 2009 to 2018 11

Table 3: Station name, country and record length of the rainfall observation 12

Table 4: Comparison of longer term ET volumes and fluxes estimated by FAO-Nile (1960–1990) and the WaPOR (2009 –2018) 15

Table 5: Comparison of longer term ET volumes and fluxes estimated by the adjusted USGS EROS SSEBop model (2005–2010) and the WaPOR (2009 –2018) 15

Table 6: Difference between storage computed from water balance and storage (GRACE) 18

Table 7: Inputs of WaterPix 23

Table 8: Outputs of WaterPix 23

Table 9: Root depth look-up table 24

Table 10: Data and calculation approach used for fluxes in WA+ Sheet 1 28

Table 11: WA+ Sheet 1 key indicators of Awash River Basin from 2010 to 2018 based on water balance derived from WaPOR datasets 33

Acronyms and Abbreviations

ΔS	Total Water Storage Change
AETI	Actual Evapotranspiration and Interception
CHIRPS	Climate Hazards Group InfraRed Precipitation with Stations
DGIS	Directorate-General for International Cooperation of the Ministry of Foreign Affairs of the Government of the Netherlands
ET_a	Actual Evapotranspiration
ET_{incr}	Incremental Evapotranspiration
ET_{rain}	Rainfall Evapotranspiration
FAO	Food and Agricultural Organization of the United Nations
GRACE	Gravity Recovery And Climate Experiment
GRanD	Global Reservoir and Dam Database
GSFC	Goddard Space Flight Center
GWF	Grey Water Footprint
IWMI	International Water Management Institute
L1_PCP_E	Level 1 Precipitation (Daily)
L1_PCP_M	Level 1 Precipitation (Monthly)
L1_RET_M	Level 1 Reference Evapotranspiration (Monthly)
L2_AETI_M	Level 2 Actual Evapotranspiration and Interception (Monthly)
L2_I_M	Level 2 Interception (Monthly)
L2_LCC_A	Level 2 Land Cover Classification (Annual)
LCC	Land Cover Classification
MLU	Managed Land Use
MWU	Managed Water Use
NASA	National Aeronautics and Space Administration
NBI	Nile Basin Initiative
P	Precipitation
PLU	Protected Land Use
Q_{out}	Flow out of the basin
TWSA	Total Water Storage Anomalies
ULU	Utilized Land Use
WA+	Water Accounting Plus
WaPOR	FAO portal to monitor Water Productivity through Open access of Remotely sensed derived data
WDPA	World Database on Protected Areas

Acknowledgements

This report was prepared by Solomon Seyoum, Bich Tran and Marloes Mul through a collaboration between IHE Delft Institute for Water Education and the Food and Agriculture Organization of the United Nations.

The report is an output of the project "Using remote sensing in support of solutions to reduce agricultural water productivity gaps" (http://www.fao.org/in-action/remote-sensing-for-water-productivity/en/), funded by the Government of The Netherlands.

Water Accounting Plus (WA+) is an approach which is based on open access data sets and information. The validation of the water accounts for the Nile River Basin depends on validation data obtained from Nile Basin Water Resources Atlas (NBI, 2017). We are therefore grateful for the Nile Basin Initiative (NBI). We would like also to acknowledge the support we received from Water Accounting group at IHE Delft including Claire Michailovsky, Bert Coerver, Abebe Chukalla, Quan Pan and Elga Salvadore. We are very grateful to Prof Graham Jewitt for his valuable comments. We also appreciated all the institutions that publish their database openly, which are all valuable for this water accounts study. These institutions/ research groups include, but not limited to, the National Oceanic and Atmospheric Administration, the World Protected Area Database and NASA's Goddard Space Flight Center (GSFC).

Executive summary

Nile River Basin is one of the largest river basins in the world with an area equivalent to 10 percent of the African continent or about 3.1 Million km^2. It is the longest river in the world at 6,695 kilometres and shared by eleven countries in north-eastern Africa and hosts more than 257 million people. The basin extends from the equatorial Plato in the south to the Mediterranean Sea in the north, crossing mountain ranges and deserts before flowing into the Nile Delta in Egypt. The climate is extremely diverse with spatially variable rainfall and evapotranspiration, creating different climatic zones. High population growth, developmental challenges and predominantly agricultural economies characterize the basin. The Nile River Basin faces a huge challenge in terms of water security. With an expected doubling of the population in the basin in the next twenty five years, water supply in the basin will be further depleted as demands for agriculture, domestic and industry continues to grow. Water availability in the basin will also be threatened by climate change and variability and pollution from increased agricultural and industrial activities and from urban areas. However, water resources of the basin are already being intensively utilised and as such the basin is considered as the one of the conflict-prone river basins.

This report describes the rapid Water Accounting Plus (WA+) study for the Nile River Basin using FAO's data portal to monitor Water Productivity through open access of remotely sensed derived data (WaPOR v2.0) database of the Food and Agricultural Organization (FAO). For this study, the WaPOR datasets for the period 2009 to 2018 were used. The WaPOR version 2.0 level 1 with 5km resolution data for precipitation and level 2 with 100m resolution data for actual evapotranspiration, reference evapotranspiration, interception and land cover classification layers were used for WA+ analyses. Additional open access data were used to assess changes in storage (the Gravity Recovery and Climate Experiment (GRACE) data). In addition, the WaPOR land cover classification layer was reclassified to WA+ classes using the World Database on Protected Areas and the Global Reservoir and Dam Database.

The analyses reveal that at basin level, between 2009 and 2019, for more than 90 percent of the time the evapotranspiration (ET_a) is greater than the precipitation (P). For specific areas, such as water bodies in the Sudan and Egypt including the Sudd wetlands and Aswan reservoir and irrigated farmlands along the banks of the river in Egypt, ET_a far exceeds P. Natural land covers also consumed huge amount of water. The difference between P and ET_a at basin level can be explained by depleting storage in the basin, however independently observed data from GRACE observed increasing storage. The error in the WaPOR water balance compared to GRACE data is 8% of P, accounting for the discrepancies between calculated and observed change in storage.

Further investigation on quality of WaPOR data per land cover classes, the values for P - ET_a in some natural land cover classes such as bare and sparse vegetation show negative values, suggesting additional water supply (incremental ET), which is unlikely. Given the sizes of these land cover classes, a small error in precipitation or evapotranspiration data hugely affects the water balance. The study also revealed that the potential for agriculture expansion in the basin is limited from a water resources perspective, even though the irrigated land accounts only for two percent of the total area. The largest proportion of the water in the basin is consumed by natural land covers. The beneficial water consumption contribution to ET_a is low compared to non-beneficial consumptions. Hence, agricultural expansion in the basin could theoretically be implemented if non-consumptive use of water by natural land covers is minimized through improvement of landscape strategies. However, such expansion should take into account the impacts of land uses changes and its impact on hydrological response of the basin, environmental flow requirements, fair share of the water resources among the riparian countries and impacts of climate variability on seasonal and periodic availability of water resources.

1. Introduction

1.1. Case study description

Nile River, called the father of African rivers, is the longest river in the world, at 6,695 km. It rises south of the Equator and flows northward through north-eastern Africa to drain into the Mediterranean Sea. The Nile Basin covers an area of about 3.1 million km², which represents about 10 percent of the African continent and contains ten major sub-basins. Eleven countries share the river: Burundi, the Democratic Republic of the Congo, Rwanda, Uganda, the United Republic of Tanzania, Kenya, South Sudan, Ethiopia, Sudan, Eritrea and Egypt. The Nile region is characterized by high population growth and significant development challenges. The Nile Basin is home to approximately 257 million people, while a total of 487 million live within the ten riparian countries (NBI, 2017; FAO, 2011), so more than 50% of the population in these riparian countries live within the Nile Basin.

The Nile basin comprises two broad sub-systems; the Eastern Nile sub-system and the Equatorial Nile sub-system. The Eastern Nile sub-system consists of the Blue Nile (Abay in the Ethiopian language Amharic) and the Atbara, which flow from the highlands of Ethiopia, and the Equatorial Nile sub-system consists of the White Nile, the headstreams of which flow into Lakes Victoria and Albert. The White Nile, originates in the Equatorial Lake Plateau (Burundi, Rwanda, Tanzania, Kenya, Democratic Republic Congo and Uganda). Other significant tributary is the Sobat, originating also in the Ethiopian highlands. These sources are located in humid regions, with an average rainfall of over 1,000 mm/year. After the confluence of these two rivers, the Nile enters the arid climate in Sudan, North Ethiopian and Egypt. The arid region starts in Sudan and extends into northern Ethiopia and Egypt.

The Nile basin comprises 10 major sub-basins (see Figure 1). The downstream stretch of the river flows northwards to the Mediterranean through the Sahara Desert. The Blue Nile flows are highly seasonal, while the White Nile waters have a steady flow and only contributes 10 to 20 percent of the total Nile runoff (FAO, 2011). At Lake Nasser, a major reservoir on the Sudan-Egypt border, the Nile River is regulated to provide water for Egypt.

It has been reported that in 2013, the Nile has a mean annual discharge of 2,800 m³/s to the Aswan Dam. The discharge is reduced to about 5 % of that amount (150 m³/s) by the time it reaches the Mediterranean Sea (GRID-Arendal, 2019). The reported annual discharge into Egypt at the Aswan dam is significantly higher than the flow which discharges to the sea, out of 88 km³/year only 5% (4.7 km³/year) reaches the Mediterranean. Other sources also estimate the discharge in to the Mediterranean Sea to be almost three times as high (13 km³/year average of the period 1984–2001) of water with or no inter-annual variability (Bouraoui et al., 2010).

The Nile sub-basins has physiographic regions with diverse characteristics such as topography, drainage patterns and geomorphology. The physiographic regions can be categorized as (1) highlands – plateaus and mountains; (2) open water surfaces (lakes – both natural and man-made); (3) wetlands and swamps; (4) flat lands; and (5) deserts (NBI, 2017). The upper sub-basin featured mainly highlands and

open surface water, and the mid and lower sub- basins mainly consists of the other three regions. The Nile River basin also contains unique features such as the Sudd wetland covering an estimated area of approximately 57,000 km², Lake Victoria (the largest natural lake in Africa), 17 wetlands sites registered by Ramsar and diverse species of flora and fauna (NBI, 2017).

1.2. Water resources developments and challenges in Nile River Basin

The Nile basin plays a very important role in the socio-economic development of the countries sharing it. Agriculture remains the backbone of the economic sector in most Nile riparian countries. Reliable access to water is key to increasing agricultural productivity, providing most of the employment, and improving living standards of the population of the Nile basin countries. The basin also has potential for hydropower generation (NBI, 2017).

High population growth and environmental degradation are affecting the Nile region. The population of Nile Basin countries, for example, grew by over four fold in the 50 years between 1960 and 2010 and consequently water, food and energy demand increased significantly. As a result, per capita water availability has been declining (NBI, 2017).

The outflow from the Nile Basin is small relative to its size. The reported outflow to the Mediterranean Sea from the basin which measures more than 3 million km² is only about 4.7 km³ /year (GRID-Arendal, 2019) and about 13 km³/year according to Bouraoui et al. (2010). NBI (2017) reports the Nile mean annual flow at Dongola, upstream of the Aswan Dam, to be 80 km³/year which is equivalent to about 30 mm depth of water over the basin area.

The upstream riparian countries have largely rural populations that depend on smallholder subsistence farming with low agricultural productivity and inefficient water use. In this part of the basin, precipitation is abundant but temporally variable. Their economy depends on the income generated from such farming and no alternative employment opportunities. Such farming practice and periodic drought occurring in the region, have been affecting food security of the region (NBI, 2017). For the downstream countries which are located in arid region with sparse precipitation, the Nile is the only significant source of water. As such the Nile flows are fully used by Egypt and the Sudan for their industrial, domestic and agricultural water supply.

The groundwater resources of Nile Basin has not been adequately studied (NBI, 2017) and literature on the subject is very limited. However, twelve trans-boundary aquifers were identified in the river basin (International Groundwater Resources Assessment Centre (IGRAC))

Groundwater exploitation in the basin differs widely from country to country where in the upstream of the basin groundwater exploitation is solely for domestic purpose while in Egypt and Sudan groundwater resources are extensible developed and used also for agriculture (MacAlister et al., 2012).

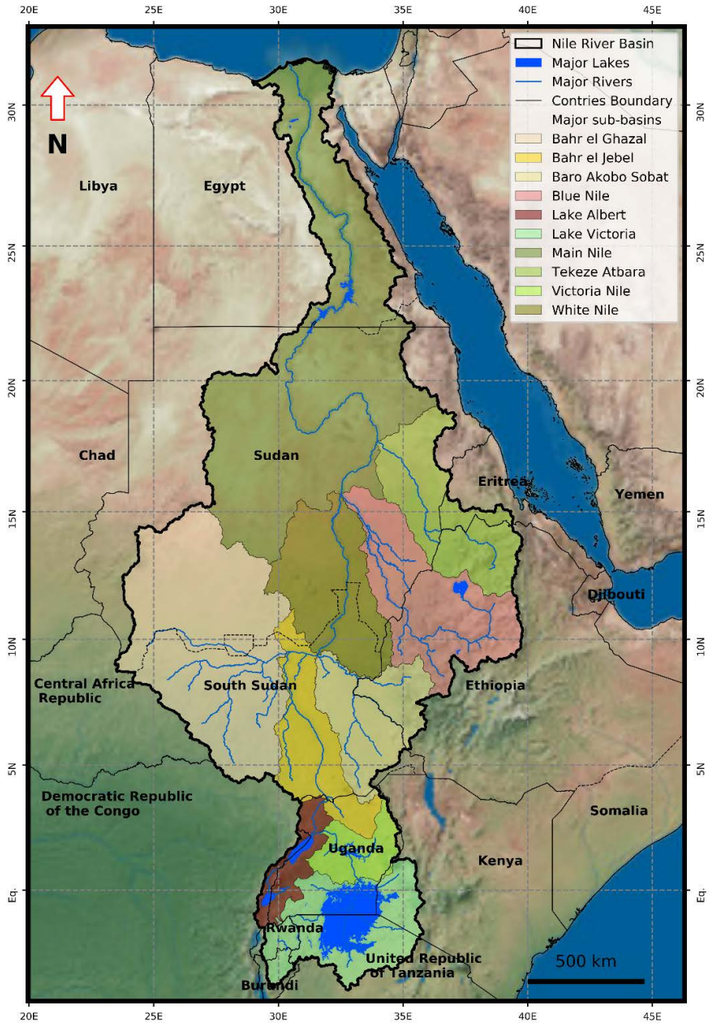

Figure 1: Location of the Nile River Basin and the ten major sub-basin of Nile (Map produced for the report using shapefile from FAO, river network from Hydroshed (Lehner and Grill, (2013), topography map from Natural Earth. Free vector and raster map data @ naturalearthdata.com and sub basins boundary from NBI, 2017

1.3. Objective of water accounts

The purpose of this study is to demonstrate how WaPOR data in conjunction with other Earth observation data sources contribute to the generation of information that provides insight in to major flows and fluxes and thereby determining water availability, withdrawals, consumptive use, non-consumptive use and the benefits and services rendered from it. In particular, the study seeks to investigate:

- What is the current water resources availability in the Nile River basin?
- How much water is being consumed by different sectors and in particular agriculture in the Nile River basin?
- What are the safe caps of water withdrawals for the agricultural sector in Nile basin?

A system referred to as Water Accounting Plus (WA+) has been designed by IHE Delft with its partners FAO and IWMI using spatial data from earth observations and various other open-access databases. It complements the lack of routine water resources data collection and incorporates spatially distributed water consumption. The WA+ framework is a reporting mechanism that summarizes the state of the water resources conditions by means of customized sheets (www.wateraccounting.org). While the WaPOR database does not contain all the input data required for fully implementing the WA+ framework, key data is provided, such as precipitation, actual evapotranspiration, the breakdown between transpiration, evaporation and interception, reference evapotranspiration, net primary production and total biomass production (FAO, 2018).

The present study shows the results of the implementation of the Water Accounting+ framework in the Nile River basin for the period 2009 to 2018 using WaPOR v2.0 data, identifying the current water challenges, the sustainable water withdrawals, and the key areas where future actions can have a profound impact. It implements a rapid WaPOR-based Water Accounting+ framework, developed for the project. It focusses on the basin-wide analyses (WA+ Sheet 1) as initial analyses of the state of the water resources utilisation in a river basin.

Finally this report reflects on the quality of the WaPOR v2.0 data for Water Accounting plus.

2. Methodology

2.1. WaPOR datasets

The WaPOR v2.0 database contains information at three different spatial resolutions. At continental level, data is available at 250m resolution (Level 1). For selected countries and basins, data is available at 100m resolution (Level 2). For detailed crop water productivity analyses for selected irrigation systems, 30m resolution data is available (Level 3). For this study we used the Level 2 (100m resolution) data. Before using the data for the Water Accounts, various checks of the data were performed such as 1) precipitation data was compared with observed rainfall data 2) water balance of the basin using WaPOR data and 3) identification of source and sink per land use classification.

2.1.1. Precipitation

WaPOR rainfall data is based on the CHIRPS database created by the United States Geological Survey (Funk et al., 2015; FAO, 2018). Figure 2 shows the spatial variability of the average annual WaPOR precipitation (P) in the Nile basin for the period 2009-2018. As it is seen clearly in the precipitation map, most of the rainfall falls in the southern parts of the basin in the Ethiopian highlands and in the Equatorial Lake Plateau. The central and north-eastern part of the basin produces little amount of rainfall.

The basin annual rainfall varied between 552 mm/year in 2009 to 724 mm/year in 2012 (Figure 3). The monthly-average precipitation shows a unimodal rainfall where most of the rainfall occurs between March and October (Figure 3). However, the pattern differs significantly across the basin with Lake Victoria basin receiving a bimodal rainfall pattern (October to December and March to May) while Ethiopia receives unimodal rainfall. The minimum monthly rainfall occurs in January (8 mm/month) and the maximum in August (121 mm/month).

2.1.2. Evapotranspiration

The WaPOR evapotranspiration (ET_a) layer estimates the total evapotranspiration, including interception. Figure 5 shows the spatial variation of ET_a in the Nile basin. Similar to the rainfall, ET_a in the southern part of the basin is significantly higher than the dryer northern part. The monthly ET_a values more or less follow the patterns of the precipitation, indicating water (through precipitation) is the main limiting factor. The ET_a in the arid region of the basin which starts in Sudan and extends into northern Ethiopia and Egypt is less than 400 mm/year. The only areas in the arid region with high ET_a values are in the irrigated areas and at dam locations such as the Aswan where the ET_a can be more than 2,400 mm/year. Open water bodies experience high evaporation losses depending on their location in the basin. Dams and lakes in the arid region experience ET_a up to 3,000 mm/year.

The inter-annual variation of basin total ET_a doesn't follow the precipitation trend. With ET_a being largely controlled (irrigation) or linked to wetland systems this is following expectations. ET_a shows a very narrow difference from year to year between the value of 690 mm/year and 726 mm/year. The annual

ET_a values are higher than annual precipitation except for the year 2012 when the precipitation is more by 25 mm/year, which mean WaPOR estimates that the basin consumes more water than it generated.

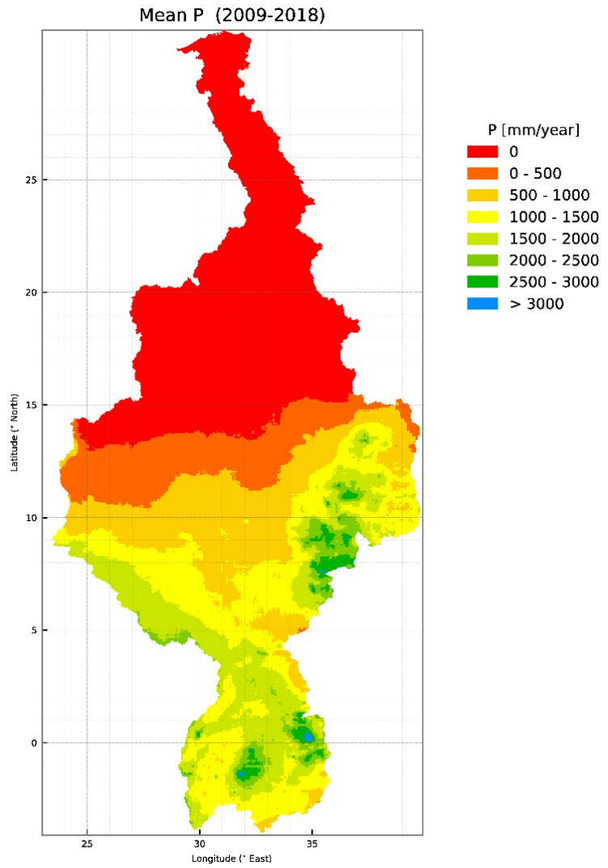

Figure 2: WaPOR annual precipitation (mm/year) for the Nile basin averaged for 2009-2018. Maps for the individual years are provided in Annex 1.

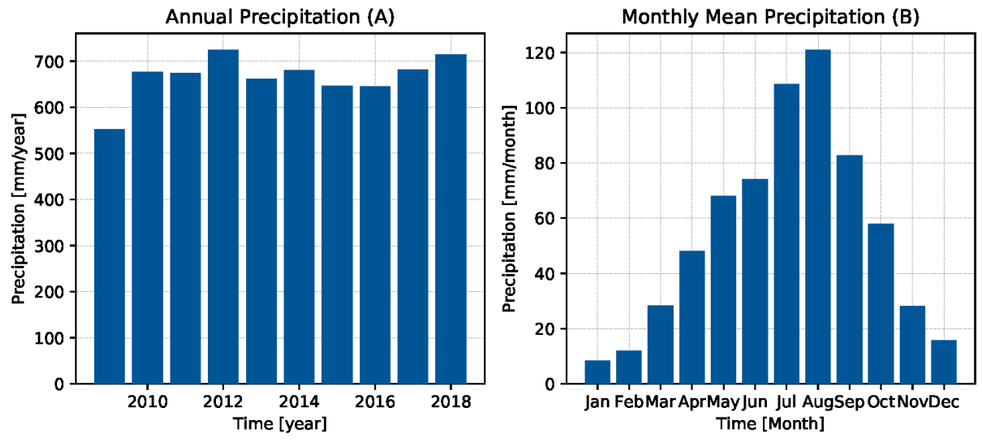

Figure 3: Annual mean (A) and monthly mean (B) WaPOR Precipitation in Nile River basin for a period of 10 years (2009 to 2018)

The monthly variation of ET_a also shows less variation than the precipitation with the minimum values of 41 mm/month in February and maximum value of 77mm/month in September.

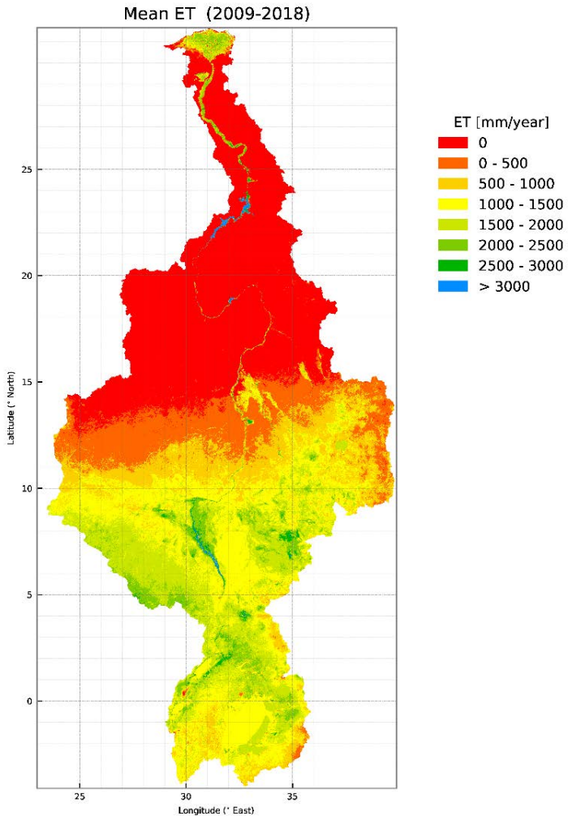

Figure 4: WaPOR annual actual evapotranspiration and interception (mm/year) for the Nile basin averaged for 2009-2018. Maps for the individual years are provided in Annex 2.

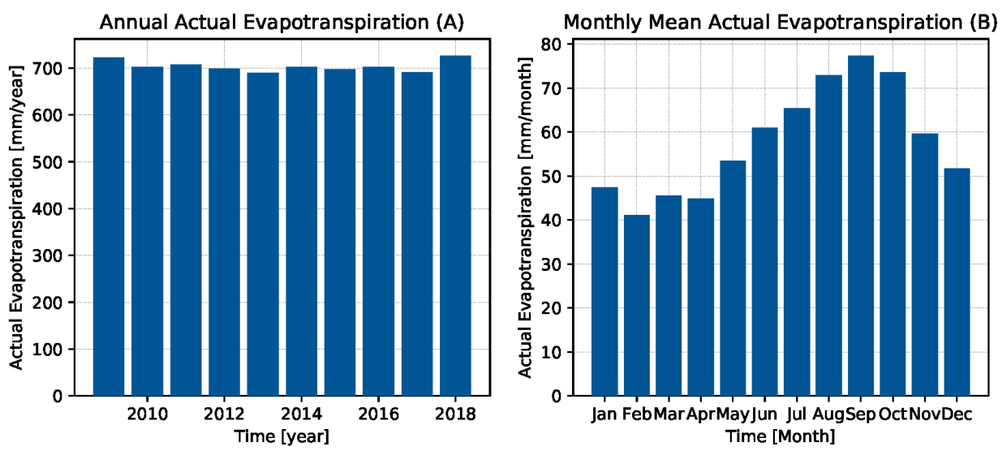

Figure 5: Annual mean (A) and monthly mean (B) WaPOR Actual Evapotranspiration in Nile River basin for a period of 10 years (2009 to 2018)

2.1.3. Precipitation minus Evapotranspiration

The WaPOR datasets for precipitation, actual evapotranspiration and interception were used to identify areas of the basin which generate water and the areas which consume water. Areas where the precipitation is more than the actual evapotranspiration and interception are considered water generating areas and those with precipitation less than the actual evapotranspiration and interception are considered as net consumers (Bastiaanssen et al., 2014). The yearly average rainfall excess or deficit (P-ET_a) for the hydrological years from 2009 to 2018 is mapped in Figure 6. As can be seen in this map, the areas generating net water are eastern part of the basin comprises the highlands of Ethiopia draining into the Tekeze Atbara and Blue Nile basins, and the southern part of the basin consists of the Equatorial Lake Plateau consisting of Lake Victoria, Victoria Nile and Lake Alberta basins.

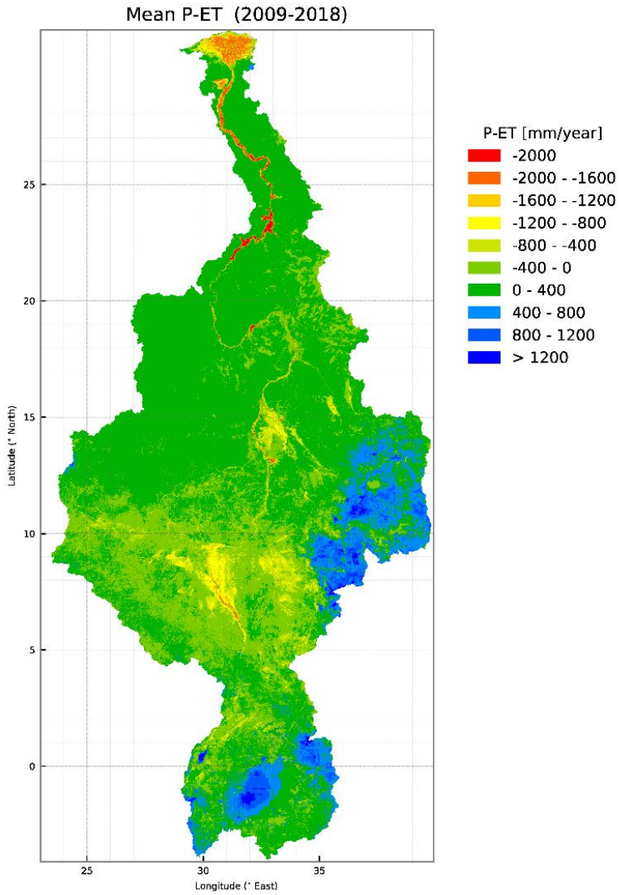

Figure 6: Precipitation minus Actual Evapotranspiration for the period 2009-2018. Maps for the individual years are provided in Annex 3.

Looking at the spatial patterns of the difference P - ET_a (Figure 6), ET_a far exceeds P in water bodies in the Sudan and Egypt such as in the Sudd wetlands, in Aswan reservoir and irrigated farmlands along the river in Egypt. P exceeds ET_a in the Ethiopian highlands and the Equatorial Plato.

To get a better sense of the basin scale water balance, for each year the P, ET_a and $P-ET_a$ values are compared (Table 1). The difference between precipitation and evapotranspiration is negative except for the year 2012 the only year in the decade from 2009 when precipitation is more than the evapotranspiration. This indicates that more water is consumed than generated in the basin by abstracting from the storage in the basin. In addition, when assuming an outflow of 4.7 km³/year the difference becomes 129.4 km³/year.

Table 1: Comparison of annual WaPOR P and ET_a values for the entire Nile Basin

Year	P (mm/year)	P (km³/year)	ET_a (mm/year)	ET_a (km³/year)	$P - ET_a$ (mm/year)	$P - ET_a$ (km³/year)
2009	552	1,698	723	2,224	-171	-526
2010	677	2,080	703	2,161	-26	-81
2011	674	2,072	707	2,172	-33	-101
2012	724	2,226	699	2,149	25	76
2013	662	2,037	690	2,120	-27	-83
2014	680	2,091	703	2,163	-23	-71
2015	647	1,989	698	2,147	-51	-157
2016	645	1,982	703	2,162	-59	-180
2017	682	2,098	691	2,124	-8	-26
2018	715	2,198	726	2,233	-11	-35
AVERAGE	666	2,047	704	2,166	-39	-118

2.1.4. Land use analysis

The WaPOR database provides a yearly land cover maps (LCC) for the Nile River Basin, which is based on the Copernicus land cover product (FAO, 2019). The land cover map of the year 2018 from the WaPOR database is presented in Figure 7. The land cover map provides 23 land use classes, with 11 different land cover classes for trees. The major land cover classes in the Nile River Basin are bare/sparse vegetation, grass land, crop land, open tries and shrub land. Throughout the study period, there were no significant changes in the area of natural land cover classes based on WAPOR data except a very small increase of rainfed croplands at the expense of irrigated croplands between 2011 and 2015. The land cover classification data may not provide a clear picture of what happened in this case as the irrigated cropland class in WaPOR's LCC layers is identified by applying a water deficit index that takes into consideration of seasonal cumulated values of precipitation and actual evapotranspiration (FAO, 2019). Bare/space vegetation land cover is the largest type with more than 30% of the total area mostly found in Egypt and northern Sudan followed by grassland with about 17%, rainfed cropland with about 15%, open tree cover about 13% and shrubland about 11%.

The water balance per land use class (Table 2) shows, as expected that irrigated croplands and flooded shrub lands consume much water followed by forests or tree covers of different types. Surplus water is mostly generated from rainfed and fallow croplands, built-up areas, and some tree cover types. Grassland in the basin generally consume blue water with evapotranspiration greater than the precipitation. Mean values of P, ET_a and their difference per each land use class is provided in Table 2.

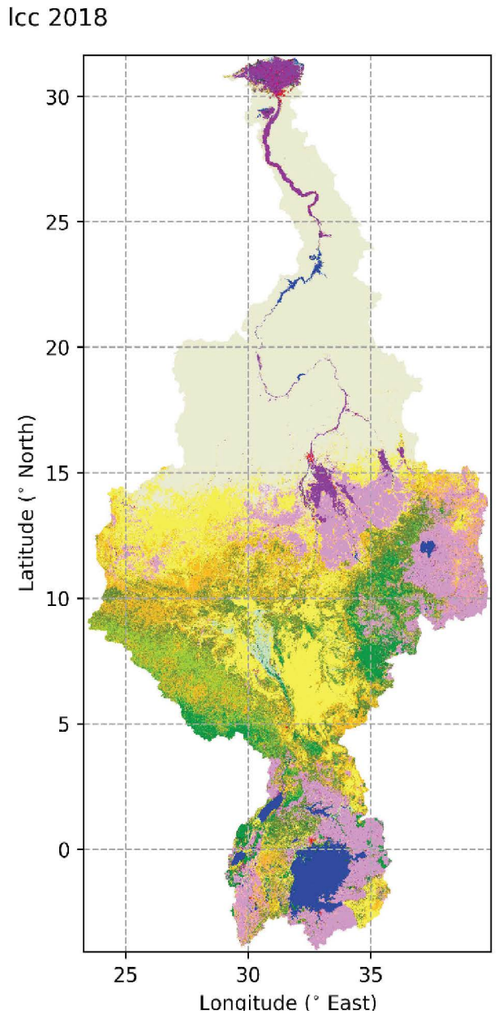

Figure 7: Land use map of the Awash Basin using WaPOR classification. Maps for the individual years are provided in Annex 4.

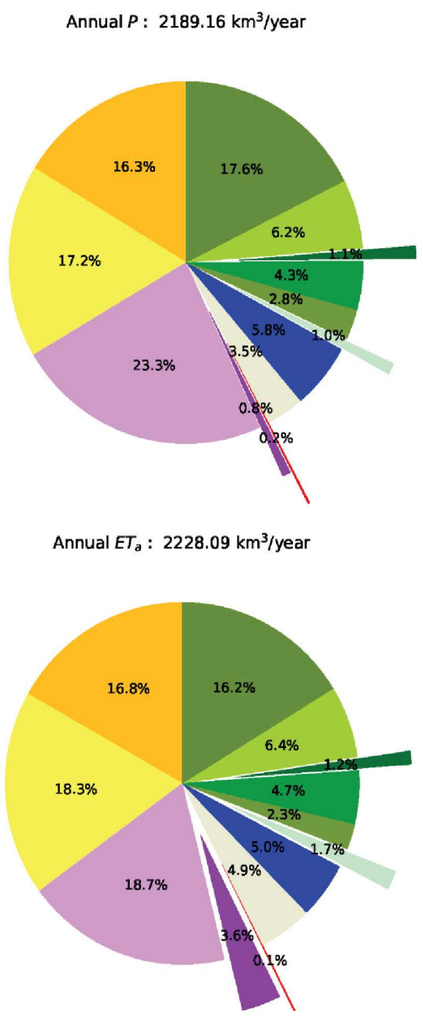

Figure 8: Contribution of the land cover classes to annual precipitation (P) and actual evapotranspiration (ET_a) of the Nile River Basin for the year 2018. The land cover classes that contribute less than 0.1% are not presented in the graphs.

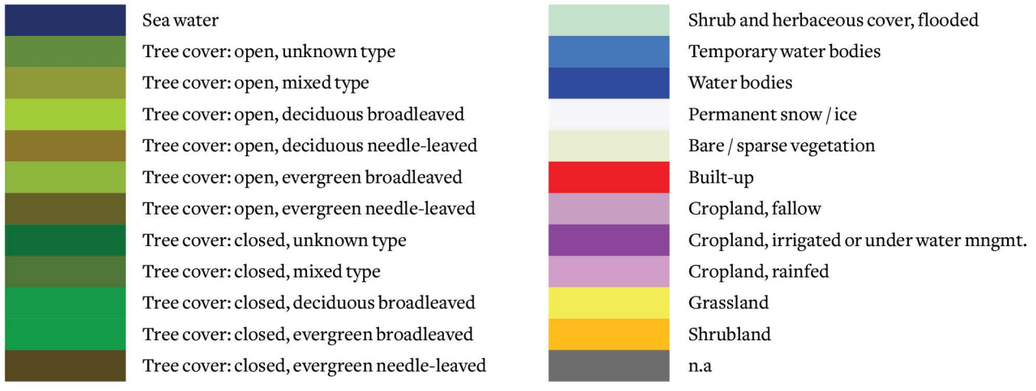

Table 2: The mean annual P - ET_a for each land cover class from 2009 to 2018 in the Nile River Basin.

Land Cover Class Description	Area (km^2)	Area (%)	P (mm/yr)	P (Mm^3/year)	ET_a (mm/year)	ET_a (Mm^3/year)	P – ET_a (mm/year)	P – ET_a (Mm^3/year)	P – ET_a
Tree cover: open, unknown type	347,607	11.31%	1,064	369,705	1,048	364,221	16	5485	1%
Cropland, rainfed	475,829	15.48%	999	475,346	880	418,544	119	56803	12%
Tree cover: open, deciduous broadleaved	103,765	3.37%	1,259	130,686	1,352	140,252	-92	-9566	-7%
Tree cover: closed, evergreen broadleaved	35,340	1.15%	1,610	56,911	1,491	52,704	119	4206	7%
Grassland	512,357	16.66%	685	350,956	762	390,351	-77	-39395	-11%
Shrubland	391,926	12.75%	859	336,638	933	365,592	-74	-28954	-9%
Tree cover: closed, unknown type	19,515	0.63%	1,225	23,905	1,349	26,317	-124	-2412	-10%
Tree cover: closed, deciduous broadleaved	68,983	2.24%	1,350	93,112	1,488	102,651	-138	-9538	-10%
Built-up	7,872	0.26%	432	3,401	484	3,811	-52	-409	-12%
Shrub or herbaceous cover, flooded	24,209	0.79%	888	21,503	1,581	38,267	-692	-16764	-78%
Tree cover: open, evergreen broadleaved	62	0.00%	1,290	80	1,435	90	-146	-9	-11%
Sea water	68	0.00%	138	9	1,339	91	-1201	-82	-873%
Cropland, fallow	2,383	0.08%	69	165	120	286	-51	-122	-74%
Water bodies	91,132	2.96%	1,259	114,752	1,216	110,792	43	3960	3%
Cropland, irrigated or under water management	66,588	2.17%	218	14,540	1,116	74,331	-898	-59791	-411%
Bare / sparse vegetation	927,123	30.15%	60	55,515	83	77,312	-24	-21797	-39%
Permanent snow / ice	2	0.00%	1,917	4	136	0	1781	4	93%
n.a	17	0.00%	170	3	58	1	112	2	66%
Total	74,779	100%	-	2,047,232	-	2,165,613	-	-118,381	-6%

2.2. Preliminary assessments

Before using the data for the Water Accounting Plus, several checks were performed including (1) comparing WaPOR data with in situ observations, (2) comparing WaPOR ET_a with other estimates for the Nile River Basin, (3) mapping net water generation and consumption and identifying net consumer land cover class, and (4) assessing WaPOR-derived basin scale water balance using remotely sensed total water storage.

2.2.1. Comparison with in situ-observations - Precipitation

Additional local validation of the precipitation was done using observed rainfall data from the basin. Long term average of rainfall for four stations in the basin namely Debre Markos in Ethiopia, Khartoum in Sudan, and Tanta in Egypt and Entebbe in Uganda were extracted from the Water Resources Atlas (NBI, 2017). The monthly rainfall values were computed from very long records of at least 100 years long except for Debre Markos which has about 48 years record (see Table 3). The results of the comparison are shown in Figure 9.

The comparison is not of the same period but the long term monthly average with the 10 year monthly average of WaPOR data. Considering this fact, it appears that WaPOR slightly underestimates precipitation with a bias value of -0.05 to 0.15 mm/month. The coefficient of correlation values vary from 0.83 to 0.99 which shows a very good agreement of monthly precipitation values from WaPOR and the four measurement locations.

Table 3: Station name, country and record length of the rainfall observation used for comparison

Station Name	Country	Record Length
Debre Markos	Ethiopia	1953-2001
Khartoum	Sudan	1900-2011
Tanta	Egypt	1904-2004
Entebbe	Uganda	1900-2006

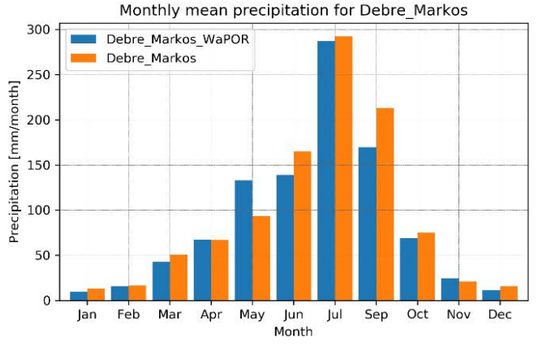

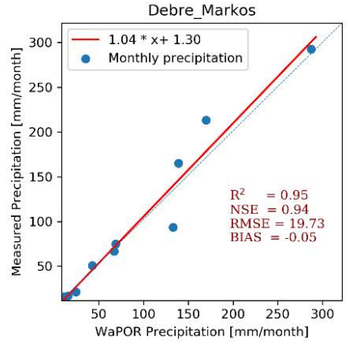

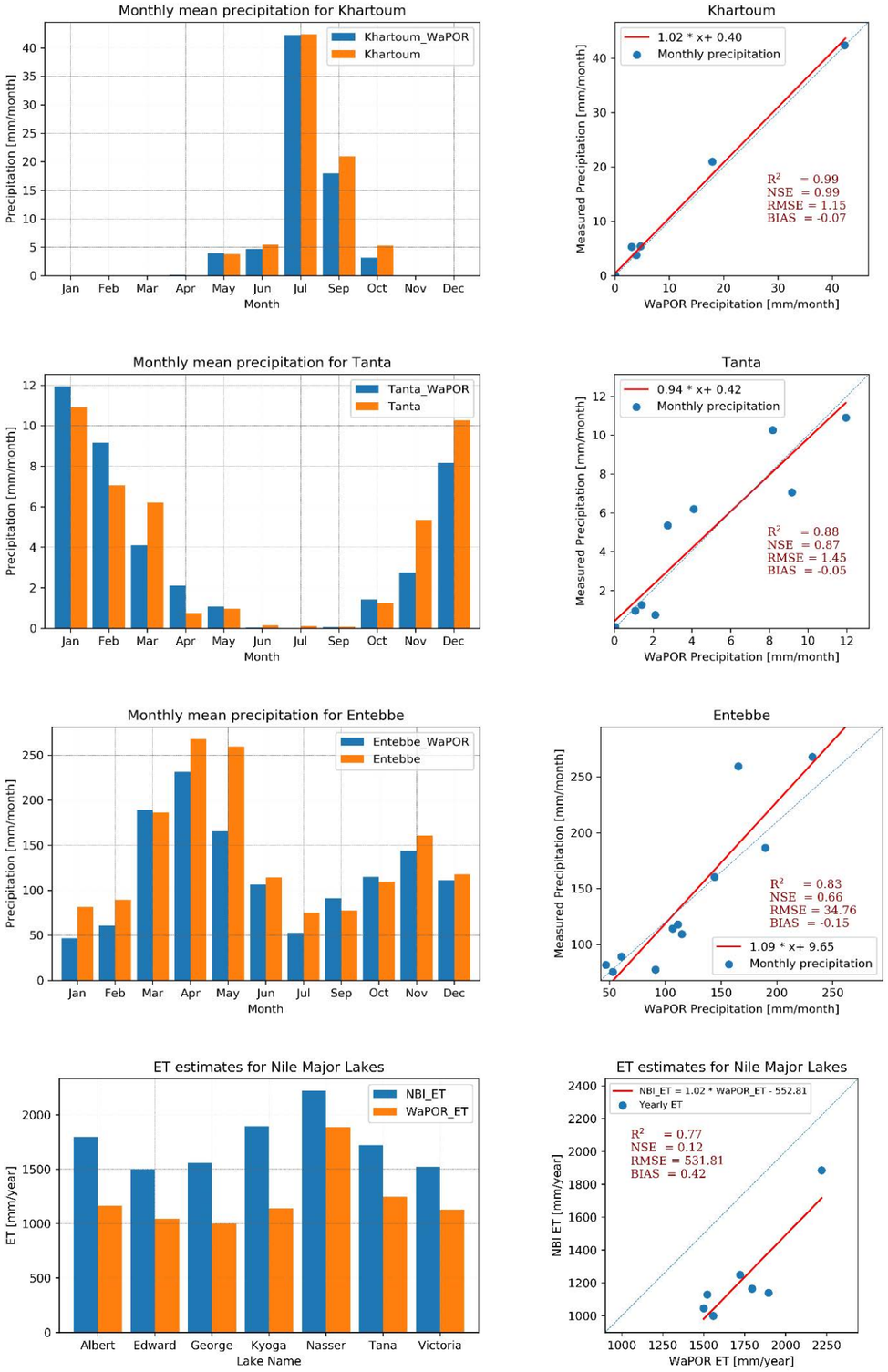

Figure 9 : Monthly WaPOR precipitation compared with rain gauges in four location in the basin at Debre Markos in Ethiopia, Khartoum in Sudan, Tanta in Egypt and Entebbe in Uganda

2.2.2. Comparison of WaPOR ET_a with other ET_a estimates for the Basin

FAO-Nile program (Hilhorst et al., 2011) and Bastiaanssen et al. (2014) have computed ET_a over the Nile Basin for different periods in the past. Though the periods over the ET_a computed are different, comparison of the ET_a flux has been made to gain insight how the WaPOR ET_a fairs with other similar estimates for the basin.

FAO-Nile program (Hilhorst et al., 2011) estimated ET_a over the Nile Basin for the period from 1960 to 1990 based on a classical water balance calculation for sub-basins. The actual ET_a over rainfed areas is calculated assuming it is equal to the reference ET_o computed on a monthly basis with the FAO Penman-Monteith method when there is enough water stored in the soil to allow actual ET_a fluxes to be equal to ET_o. When there is no enough water stored in the soil to allow this, a soil moisture reduction term is used. For irrigated areas identified from the land use map derived from FAO's AQUASTAT, ET_a was assumed to be equal to ET_o after correction with a crop coefficient. Evaporation from open water and wetlands was estimated from ET_o and calibrated through closure of the water balance.

Bastiaanssen et al. (2014) produced yearly estimates ET_a maps for Nile Basin for the period 2005 to 2010 based on the Operational Simplified Surface Energy Balance (SSEBop) model, developed and tested by U.S. Geological Survey Earth Resources Observation and Science (EROS) Center adjusted using ET Look model developed by Bastiaanssen et al. (2014) results. The SSEBop ET_a product they used has a pixel dimension of 1 km and computes the surface energy balance on the basis of thermal infrared measurements by the MODIS satellite.

The boundaries of the Nile sub-basin used by the FAO_Nile program is slightly different from the one used for this study. Also the boundaries used by Bastiaanssen et al (2014) is different from both the boundaries used by FAO Nile program and this study. Therefore, the ET_a values estimated using the three approaches are compared ET flux instead of volume. Table 4 and Table 5 show the comparison of WaPOR ET_a versus FAO-NILE estimates and WaPOR ET_a versus ET_a produced in Bastiaanssen et al. (2014).

The FAO-Nile program estimated the mean ET_o to be 628 mm/year while the WaPOR ET_o is 704 mm/year showing almost 12% increase from the FAO-Nile ET_o. Except for two sub-basin, WaPOR ET_o estimates are higher than the FAO-Nile estimate. WaPOR ET_o estimates for Blue Nile and Lake Victoria are less than the FAO-Nile estimates by 2% and 8% respectively. The maximum change is observed for Baro Akobo Sobat sub-basin at 35% followed by White Nile at 22% and Bahr el Ghazal at 17.5%.

Bastiaanssen et al. (2014) estimate the mean ET_o to be 616 mm/year with a difference 14% with WaPOR ET_o. The largest difference is for Victoria Nile - Lake Albert sub basin with 23.2% followed by Baro Akobo Sobat sub-basin with 21%.

The ET_o comparisons showed that WaPOR ET_o are higher on average than the two ET_o products. However since the approach, the period over the ET_o is computed (for FAO-Nile from 1960-1990, for the Adjusted SSEBop Model from 2005 to 2010 and for WaPOR 2009 to 2018) and the resolutions of the data used (for the Adjusted SSEBop Model 1 km and for WaPOR 100 m) are different, it is not possible to infer the reasons for the increase in WaPOR ET_o other than that WaPOR includes evaporation from interception while SSEBop does not.

Table 4: Comparison of longer term ET volumes (km³/year) and fluxes (mm/year) estimated by FAO-Nile (1960–1990) and the WaPOR (2009 –2018)

FAO-Nile				WaPOR				
Description	**Area** (km²)	**ET_a** (km³/year)	**ET_a** (mm/year)	**Description**	**Area** (km²)	**ET_a** (km³/year)	**ET_a** (mm/year)	**Dev.** (%)
Main Nile d/s Atbara	877,866	109	124	Main Nile	856,494	121	141	-13.9
Atbara	237,044	94	397	Tekeze Atbara	237,136	105	444	-11.8
Main Nile d/s Khartoum	34,523	7	211					
Blue Nile	308,198	266	863	Blue Nile	306,970	260	847	1.9
White Nile	260,943	145	554	White Nile	259,895	176	676	-22.0
Bahr el Ghazal & el Arab	606,428	454	749	Bahr el Ghazal	601,915	530	880	-17.5
Pibor-Akabo-Sobat	246,779	224	907	Baro Akobo Sobat	201,192	246	1,224	-35.0
Bahr el Jebel	136,400	163	1,196	Bahr el Jebel	186,338	239	1,282	-7.2
Kyoga-Albert	197,253	224	1,124	Victoria Nile – L. Albert	161,315	208	1,289	-14.7
Lake Victoria basin	264,985	308	1,160	Lake Victoria	263,020	281	1,067	8.0
Total and average	**3,170,419**	**1,991**	**628**		**3,074,273**	**2,165**	**704**	**-12.2**

Table 5: Comparison of longer term ET volumes (km³/year) and fluxes (mm/year) estimated by the adjusted USGS EROS SSEBop model (2005–2010) and the WaPOR (2009 –2018)

Adjusted SSEBop Model				WaPOR				
Description	**Area** (km²)	**ET_a** (km³/year)	**ET_a** (mm/year)	**Description**	**Area** (km²)	**ET_a** (km³/year)	**ET_a** (mm/year)	**Dev** (%)
Main Nile 1,2,3	98,3375	106	107	Main Nile	856,494	121	141	-13.9
Tekezze-Atbara	231,492	105	453	Tekeze Atbara	237,136	105	444	-11.8
Main Nile 4	35,338	6	180					
Blue Nile	307,262	226	737	Blue Nile	306,970	260	847	1.9
Lower White Nile	237,429	146	617	White Nile	259,895	176	676	-22.0
Bahr el Ghazal - Sudd	717,069	655	913	Bahr el Ghazal	601,915	530	880	-17.5
Baro-Akobo-Sobat	230,369	233	1012	Baro Akobo Sobat	201,192	246	1,224	-35.0
Albert Nile-Bahr - al Jabal	80,433	92	1144	Bahr el Jebel	186,338	239	1,282	-7.2
Victoria Nile - L.Albert	156,839	164	1047	Victoria Nile – L. Albert	161,315	208	1,289	-14.7
Lake VictoriaKagera	249,433	254	1018	Lake Victoria	263,020	281	1,067	8.0
Total and average	3,229,039	1,988	616		3,074,273	2,165	704	-14.3

2.2.3. Comparison with other remote sensing estimates - Actual Evapotranspiration and Interception

The NBI has produced estimates of ET_a over the whole of the Nile Basin at a resolution of 1 km² at 8-day time step. This dataset covers from January 2000 to 2014 (Nile Waters, 2014), using an improved algorithm from the global MOD16ET algorithm which uses daily meteorological data and MODIS land surface dynamic datasets as inputs for daily ET calculations[1].

In particular, the NBI ET_a estimates were compared with the average annual WaPOR evapotranspiration and interception for lakes in the basin, as IHE Delft (2020a) found issues with the ET_a for water bodies in the Jordan River Basin. Figure 9 shows the result of this comparison. The WaPOR ET_a estimates are significantly lower than the NBI estimates for all the lakes. The NBI ET_a estimates are 17 to 66 % higher than that of WaPOR where the biggest difference is for Lake Kyoga followed by lakes George and Alberta.

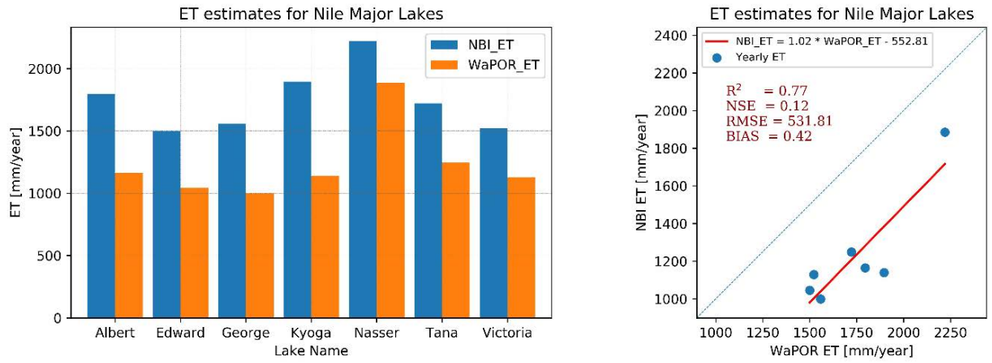

Figure 10: Comparison of annual ET_a estimates of NBI and WaPOR for major lakes on Nile River Basin

2.2.4. Conclusion

The preliminary data quality assessments shows that WaPOR 2.0 Level 2 data provides reasonable estimates of WaPOR P and ET_a at basin scale and as such can be useful to map the general spatial distribution and identify areas of net water generation and water consumption in the basin. In general, spatial variation of P and ET_a are consistent with the characteristics of the basin.

However, when WaPOR P compared with gauge measurements, slight underestimation has been observed at all the four stations used for the comparison. Though there are several precipitation measurement stations in the river basin, the data were inaccessible for this study and therefore it was not possible to generalize if the underestimation of WaPOR P is valid for the whole basin. Also, for large parts of the basin, no validation precipitation data set is available, in particular in the areas where we

1 http://nileis.nilebasin.org/category/wr-data/hydrology/evapotranspiration

found discrepancies in $P-ET_{a,}$ such as in the shrubs and bushlands. The comparison of annual ET_a of major lakes in the basin also showed significant under estimation, therefore for further analysis, the ET_a for water bodies is replaced with ET_{ref}.

The comparison of WaPOR P and ET_a, shows that, except for the year 2012, ET_a is higher than P. This may indicate that water storage in the basin was being depleted or there may be issues with the values of either or both P and ET_a.

The annual ET_a for the period 2009-2017 from WaPOR v2.0 Level 2 (702 mm/year) is higher than the ET_a for the period 2009-2017 from WaPOR v1.0 Level 1 (668 mm/year) (Table 13; FAO and IHE Delft, 2019). The estimation of ET_a from the water balance $(P-Q)$ for the period 1912-1984 based on observations is 667 mm/year, similar to WaPOR v1.0 Level 1. For the newer WaPOR v2.0, the difference is larger, however it must be noted that the comparisons are done using datasets from different time periods, and the difference may be due to regular climatic variability.

2.3. Other global data sets

2.3.1. GRACE

To assess how much of the difference between P and ET_a is due to groundwater outflow and change in storage we use the Gravity Recovery and Climate Experiment (GRACE), a dual-satellite mission continuously monitoring and mapping Earth's changing gravity field to estimate the total water storage anomalies (TWSA). There are several GRACE solutions for TWSA estimation from gravity anomalies, which covers the whole globe from 2003 till end of 2015. The GSFC-v02.4-ICE6G solution (Luthcke et al., 2013) was used to validate the assumption that storage change over a longer time scale such as hydrological year should be zero or close to zero. Though, GRACE solution provides mean monthly TWSA, the number of days may not exactly match the days of the months and as such the change in storage ($\Delta S/\Delta t$) in a time period was approximated using a second order central difference as proposed by Biancamaria et al. (2019). After that, $P-ET_a$ should be equal to the total outflow Q_{out}, after correction in change of storage ($\Delta S/\Delta t$) following the water balance equation:

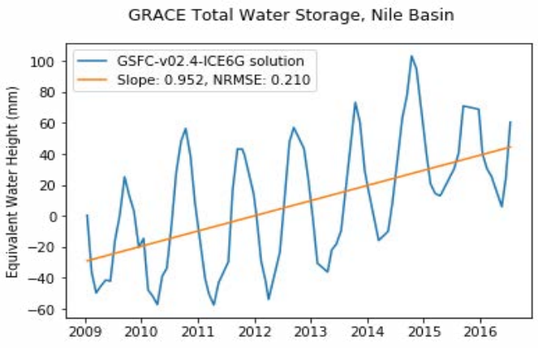

Figure 11: Longer term trend of increasing water storage in Awash Bain on GRACE gravity measurements (source: *https://ccar.colorado.edu/grace/gsfc.html*)

The longer term trend in storage change (ΔS) as observed by GRACE is positive (see Figure 11). The trend of water storage for a number of GRACE pixels that cover Nile River Basin from 2009 to 2016 is 0.95 mm/year, which is translated into 2.8 km³/year. The increase in trend in change in storage may be a result of the construction of a number reservoirs, which then store water.

2.3.2. Errors in water balance

The difference between residual $P-ET_a-Q_{out}$ and ΔS can be used as a proxy of error in water balance derived from available datasets. The errors could be due to uncertainty in WaPOR P and ET_a, assumption of the outflow discharge (Q_{out}) and/or from GRACE TWSA solution. For the Nile River Basin, $P-ET_a-Q_{out}$ is computed using the assumed yearly outflow from the basins of 4.7 km³/year.

Table 6: Difference between storage computed from water balance and storage from GRACE

Year	P (km³/year)	$P-ET_a-Q_{out}$ (km³/year)	ΔS Grace (km³/year)	Error (mm/year)	Error as% of P (km³/year)
2009	1,698	-530	24	-555	-33
2010	2,080	-85	-64	-21	-1
2011	2,072	-106	27	-132	-6
2012	2,226	72	44	27	1
2013	2,037	-88	-8	-80	-4
2014	2,091	-76	53	-129	-6
2015	1,989	-162	92	-254	-13
AVERAGE	2,028	-139	24	-163	-8

On average, the mean difference between GRACE TWSA change and WaPOR-based JS is -8% of total precipitation volume (Table 6). The error is the largest for 2009 with -33% while it is only 1% for year 2012. The error in water balance seem related with the amount of precipitation the basin received. Figure 12 show a linear relationship between errors in water balance the precipitation.

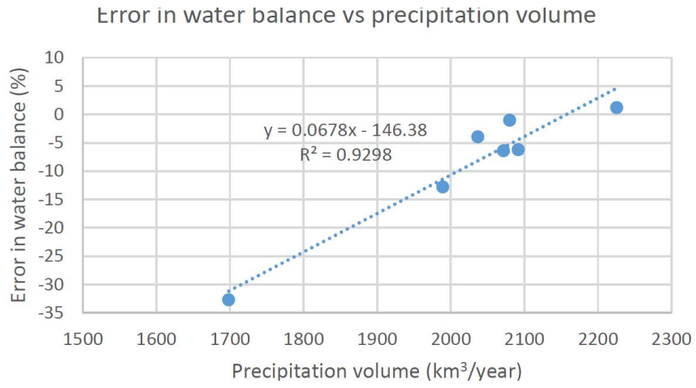

Figure 12: Error in water balance vs precipitation volume

2.3.3. Global maps to categorise land use classes

The land use map forms the basis for dividing the basin landscape into the four main categories (PLU, ULU, MLU, MWU). Four main categories of land and water uses are distinguished:

- Protected Land Use (**PLU**); areas that have a special nature status and are protected by National Governments or Internationals NGO's
- Utilized Land Use (**ULU**); areas that have a light utilization with a minimum anthropogenic influence. The water flow is essentially natural
- Modified Land Use (**MLU**); areas where the land use has been modified. Water is not diverted but land use affects all unsaturated zone physical process such as infiltration, storage, percolation and water uptake by roots; this affects the vertical soil water balance
- Managed Water Use (**MWU**); areas where water flows are regulated by humans via irrigation canals, pumps, hydraulic structures, utilities, drainage systems, ponds etc.

The underlying reason for framing these four land use categories is that their management options widely differ from keeping them pristine to planning hourly water flows.

The land use categories map (Figure 13) is based on the land cover layer (LCC) from WaPOR database, but needed to be reclassified into the Water Accounting classes. Protected Land Use (PLU) class was updated using the protected area profile from the World Database on Protected Areas (UNEP-WCMC, 2019). The areas which are designated as IUCN categories Ia (strict nature reserve), Ib (wilderness area) and II (national park) are reclassified as PLU. The Managed Water Use class was reclassified from the 'Cropland, irrigated or under water management' and 'Built-up' classes in WaPOR LCC layer and updated with the area of constructed reservoirs from the Global Reservoir and Dam Database (GRanD) (Lehner et al., 2011). WaPOR water bodies class except for natural lakes were also reclassified as Managed Water Use class. The Modified Land Use was reclassified from the class 'Cropland, fallow' and 'Cropland, rainfed' in the WaPOR LCC layer. Thereafter, the rest of the area was reclassified as Utilized Land Use class.

The land use class used for year 2018 in the analyses is shown in Figure 13. The majority of the area in the Nile River Basin is covered by utilised land use and modified land use.

2.4. WA+ methodology

The longer term planning process of water and environmental resources in river basins requires a measurement – reporting – monitoring system in place. The Water Accounting Plus (WA+) framework is based on the early WA work of Molden (1997) focussing on agriculture and irrigation systems. WA+ was further developed by Karimi (2014) and Karimi and Bastiaanssen (2015)and not generally accessible. Remote sensing data is a suitable alternative to measure the required input variables. This paper reviews the reliability of remote sensing algorithms to accurately determine the spatial distribution of actual evapotranspiration, rainfall and land use. For our validation we used only those papers that covered study periods of seasonal to annual cycles because the accumulated water balance is the primary concern. Review papers covering shorter periods only (days, weeks for river basin analyses and incorporating of all water use sectors. Further developments include more hydrological and water management processes and focus on specific land uses.

A key element of WA is that it separates ET_a into Rainfall ET (ET_{rain}) and incremental ET (ET_{incr}), thereby clearly identifying managed water flows. WA+ includes thus the hydrology of natural watersheds that provide the mains source of water in streams and aquifers, as well as quantifying water consumption. The current study utilises the WaPOR v2.0 Level 2 data (100 m resolution) for the analyses. It presents a rapid WaPOR-based water accounting framework.

The output of WA+ is in a number of sheets and supporting spatial maps. Remote sensing, GIS and spatial models form the core methodology, so all data has a spatial context. The accounts are reported on an annual basis, as WA+ is meant for longer term planning. Software tools have been developed that automatically collect and download data from WaPOR database as well as for the calculations. The models and scripts for the creation of the water accounts and the elaboration of the reports are available on GitHub under the Water Accounting account[2]. The WA+ framework is public and open for all users.

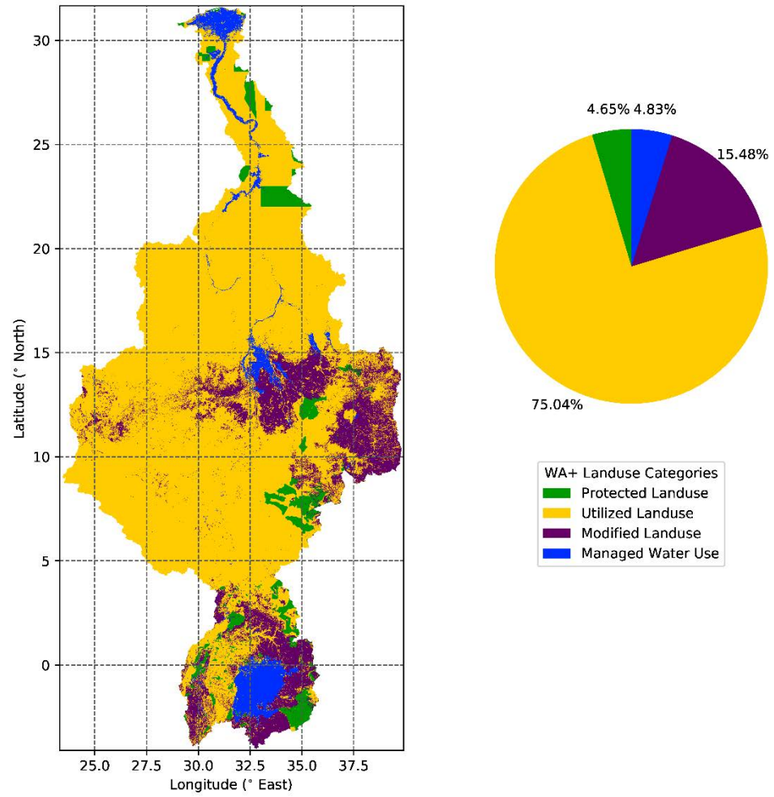

Figure 13: Area percentage of WA+ Land Use categories in Nile River basin in 2018

2 https://github.com/wateraccounting

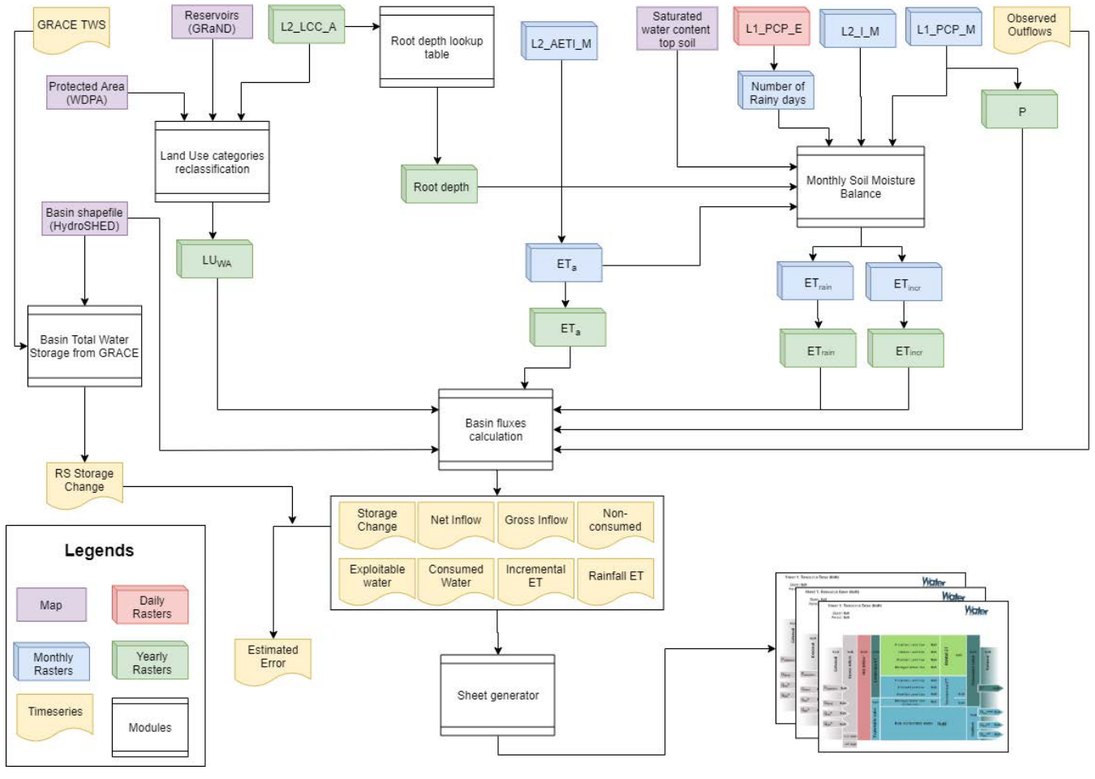

Figure 14: Water accounting flow chart using WaPOR data

Figure 14 shows the flow chart of the water accounting process and the data used to develop the water accounting for Nile River Basin. It mainly uses WaPOR data such as the level 1 monthly precipitation and level 2 annual time series of land cover classification, interception and actual evapotranspiration and interception. External data sources used include GRACE satellite data for estimating the change in storage in the basin, Global Reservoir and Dam Database (GRanD) to identify dam locations and extents, and the World Database on Protected Areas to identify the protected land uses.

2.4.1. Pixel scale analysis

2.4.1.1. Method

The water accounting framework distinguishes between a vertical and horizontal water balance. A vertical water balance is made for the unsaturated root zone of every pixel and describes the exchanges between land and atmosphere (i.e. rainfall and evapotranspiration) as well as the partitioning into infiltration and surface runoff. Percolation and water supply are also computed for every pixel, to facilitate attributing water supply and consumption to each land use class.

The WaterPix model calculates for each pixel the vertical soil water balance (See Figure 15) and is described below. ET_{rain} and ET_{incr} are separated by keeping track of the soil moisture balance and determining if ET is satisfied only from rainfall or stored in the soil moisture or additional source (supply) is required. The main inputs into WaterPix are provided in Table 7 and the outputs are provided in Table 8. Each parameter is calculated at the model resolution of 100m and available for monthly and annual time steps.

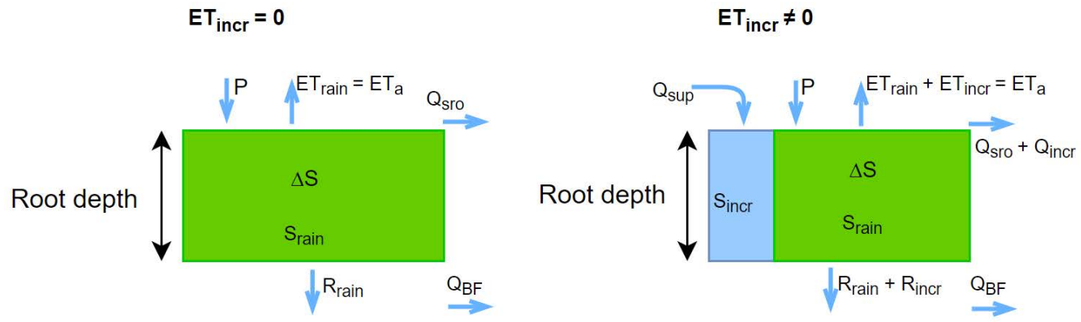

Figure 15: Main schematization of the flows and fluxes in the WaterPix model

Table 7: Inputs of WaterPix

Variable	Parameter	Source	Spatial Resolution	Temporal resolution
Precipitation	P	WaPOR	5,000 m	Daily
Actual Evapotranspiration	ET_a	WaPOR	100 m	Monthly
Interception	I	WaPOR	100m	Monthly
Land cover map	LULC	WaPOR	100 m	Yearly
Saturated Water Content		HiHydroSoil	0.008333 degree (about 900m at the equator)	Static

Table 8: Outputs of WaterPix

Variable	Calculation step	Definition
S	1	Soil Moisture
Q_{sro}	1,4	Surface Runoff
R	1,4	Recharge
ET_{rain} and ET_{incr}	2	Rainfall and incremental ET
Q_{sup}	3	Supply

Step 1: Compute soil moisture

The soil moisture ($S_{rain,t}$) is computed as the soil moisture storage at the end of the previous timestep ($S_{rain,t-1}$) plus the effective rainfall ($P-I$) minus recharge (R_{rain}) and surface runoff (Q_s) (eq.):

$$S_{rain,t} = S_{rain,t-1} + P - I - R_{rain} - Q_{sro,rain} \quad \text{(eq. 1)}$$

Where the surface runoff ($Q_{sro,rain}$) is calculated using an adjusted version of the Soil Conservation Service runoff method. The adjusted version replaces the classical Curve Numbers by a dynamic soil moisture deficit term that better reflects the dry and wet season infiltration versus runoff behaviour (see Schaake et al., 1996; Choudhury and DiGirolamo, 1998). As the Curve Number method is developed for event based runoff, we calculated $Q_{sro,rain}$ on daily basis, dividing the effective rainfall by the number of rainy days (n) and a calibration parameter to account for the soil moisture variation due to drying up and filling with in a month. The total surface runoff for a month is then multiplied by n:

$$Q_{sro,rain} = \begin{cases} 0 \text{ if } P = 0 \\ \dfrac{\left(\dfrac{P-I}{n}\right)^2}{\dfrac{P-I}{n} + f(S_{sat} - S_{rain,t-1})} * n \text{ if } P \neq 0 \end{cases} \quad \text{(eq. 2)}$$

Where the saturated soil moisture (is calculated by multiplying the Saturated Water Content (θ_{SAT}) by the effective root depth (RD) for each land cover class estimated based on the effective root depth by Yang et al. (2016) (Table 9).

Table 9: Root depth look-up table. The values of root depth for each land cover class is based on study by Yang et al. (2016)

WaPOR Land cover class	Root depth (mm)
Shrubland	370
Grassland	510
Cropland, rainfed	550
Cropland, irrigated or under water management	550
Fallow cropland	550
Built-up	370
Bare/sparse vegetation	370
Permanent snow/ice	0
Water bodies	0
Temporary water bodies	0
Shrub or herbaceous cover, flooded	0
Tree cover: closed, evergreen needle-leaved	1,800
Tree cover: closed, evergreen broad-leaved	3,140
Tree cover: closed, deciduous broad-leaved	1,070
Tree cover: closed, mixed type	2,000
Tree cover: closed, unknown type	2,000
Tree cover: open, evergreen needle-leaved	1,800
Tree cover: open, evergreen broad-leaved	3,140
Tree cover: open, deciduous needle-leaved	1,070
Tree cover: open, deciduous broad-leaved	1,070
Tree cover: open, mixed type	2,000
Tree cover: open, unknown type	2,000
Seawater	0

Step 2: Separate ET_a into ET_{rain} and ET_{incr} and update S

To compute the rainfall and incremental component of ET, ET_a is subtracted from $S_{rain,t}$. When $S_{rain,t}$ is insufficient for ET_a, the difference will be supplied by surface or groundwater uptake. The rainfall ET (ET_{rain}) becomes the amount which can be supplied by the soil moisture, whereas the difference will become ET_{incr}:

$$ET_{rain} = if(S_{rain,t} > ET_a, ET_a, S_{rain,t}) \quad \text{(eq. 3)}$$

$$ET_{incr} = ET_a - ET_{rain} \quad \text{(eq. 4)}$$

The new soil moisture storage then becomes:

$$S_{rain,t} = S_{rain,t} - ET_{rain} \quad \text{(eq. 5)}$$

Step 3: Estimation of Water Supply

The amount of water supplied to each pixel is a function of ET_{incr} and the so called consumed fraction (f_c).

$$Q_{sup} = f(ET_{incr}, LU) = \frac{ET_{incr}}{f_c} \quad \text{(eq. 6)}$$

f_c is dependent on the land use class and was suggested to replace the classical irrigation efficiencies (Molden, 1997; Simons et al., 2016).

The consumed fractions applied in this study are only for irrigated crops with a consumed fraction (fc) of 0.80.

Step 4: Estimating incremental soil moisture

A separate soil moisture storage (blue area in Figure 15) is added to store Q_{sup} and calculate incremental recharge and runoff as follows:

$$S_{incr,t} = S_{incr,t-1} + Q_{sup} - ET_{incr} - R_{incr} - Q_{sro,incr} \quad \text{(eq. 7)}$$

And total soil moisture storage (S_t) becomes:

$$S_t = S_{rain,t} + S_{incr,t} \quad \text{(eq. 8)}$$

Then total recharge (R_t) is calculated as exponential function of the soil moisture. If the soil moisture is above a certain percentage (calibration parameter) of the saturated content, the percolation will be computed using the following simple exponential function:

$$R_t = S_t * exp\left(- \frac{1}{S_t}\right) \quad \text{(eq. 9)}$$

And the incremental recharge () and the recharge from rainfall (are computed as proportions of the incremental and rain soil moisture values.

The surface runoff is updated to account the increase due to incremental surface runoff from the supply

$$Q_{sro\,tot} = \frac{\begin{cases} 0 \text{ if } P = 0 \\ \left(\frac{P + Q_{sup} - I}{n}\right)^2 \end{cases}}{\frac{P + Q_{sup} - I}{n} + f(S_{sat} - (S_{rain,t} + S_{incr}))} * n \text{ if } P \neq 0 \text{ or } Q_{sup} \neq 0 \quad \text{(eq. 10)}$$

The incremental surface runoff ($Q_{sro,incr}$) is then computed as:

$$Q_{sro,incr} = Q_{sro,tot} - Q_{sro,rain} \quad \text{(eq. 11)}$$

The results of the calculation for ET_{rain} and ET_{incr} for the different land use classes are shown in Figure 16. It shows that irrigated cropland, flooded shrub land, shrub land, built-up, grassland and water bodies have the highest ET_{incr}. For irrigated croplands the method estimates ET_{incr} to be about 408% of the precipitation. This shows that about 80% of the water used by irrigated crops comes from supply other than precipitation, this is mainly the case in the irrigated areas in Egypt with very little rainfalls. For flooded shrub land this amount is 168%. An unusual situation for Nile basin is that the built-up areas also have higher ET_{incr} as opposed to generating flow as shown in other basin such as Awash River basin (FAO and IHE Delft, 2020) and Niger River Basin (FAO and IHE Delft, 2020b).

Figure 16 also shows that two natural land use classes appear to consume more than the precipitation. Grass land consumes 8% more than the precipitation and bare/sparse vegetation consumes 37% more than precipitation. The excess of 23mm/year for bare/sparse vegetation and 59 mm/year for grassland are not excessively high values but accumulating to large discrepancy in the overall water balance. These excesses can be translated less than 1.5 mm/day in decadal ET_a or less than 0.15 mm of daily P values.

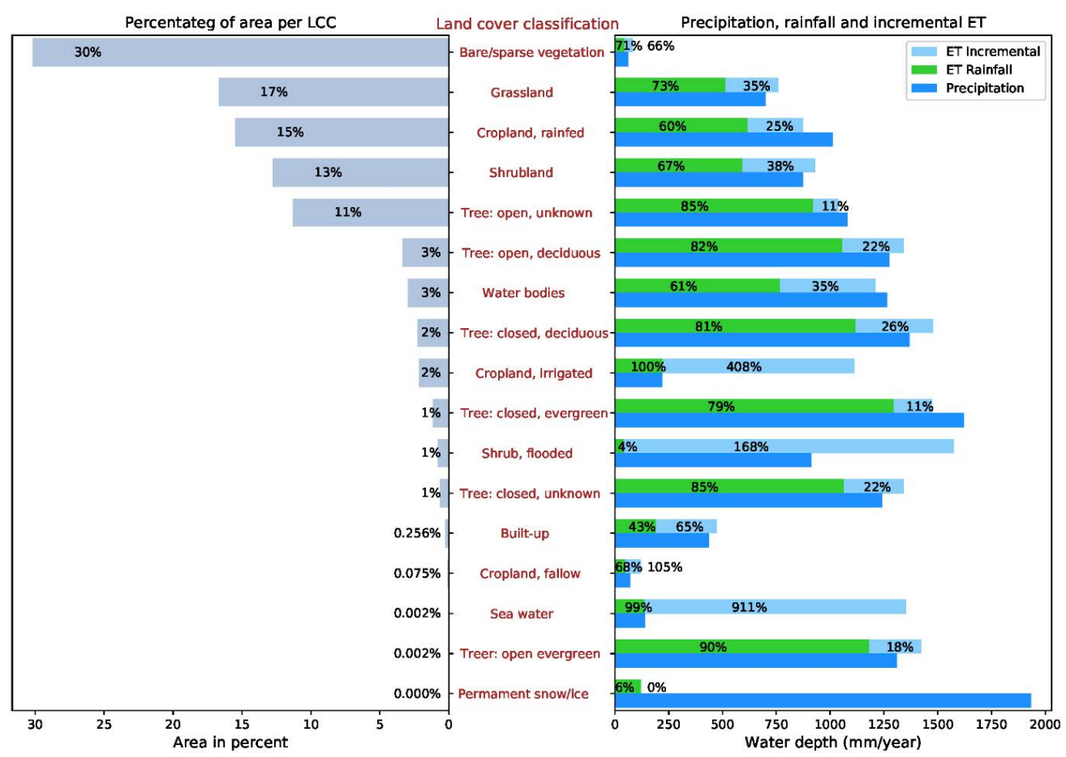

Figure 16: Precipitation, ET_{rain} and ET_{incr} per land cover of Nile River Basin for the period 2010 to 2018 - the percentages indicate the proportion of ET_{rain} and ET_{incr} to the precipitation

2.4.2. WaPOR based Water Accounting Plus sheet 1

The water accounts sheet 1 provide an overview of the water resources and its current utilisation per different land use categories. The rapid WaPOR-based Water Accounting looks at the gross inflow, rainfall and incremental evapotranspiration for each of the WA+ land use categories. It assesses the current utilisation rate of a river basin.

A further analysis was done, using a set of key indicators for water accounting developed by Dost et al (2013) in consultation with the Land and Water Division of FAO:

The first set of indicators can be related to the Resource Base Sheet:

1. $ET\ Fraction = \frac{ET_{tot}}{(P + Q_{in})}$ (%)

   ET fraction indicates which portion of the total inflow of water is consumed and which part is converted into renewable resources. A value higher than 100% indicates over- exploitation or a dependency on external resources.

2. $Stationarity\ Index = \frac{\Delta\ Storage}{ET_a}$ (%)

   Stationarity Index is an indication of the depletion of water resources. Positive values indicate that water is added to the groundwater and/or surface water storage. Negative values indicate a depletion of the storage.

3. $Basin\ Closure = \frac{1 - Outflow}{(P + Q_{in})}$ (%)

   Basin Closure defines the percentage of total available water resources (Precipitation + basin inflow) that is consumed and/or stored within the basin. A value of 100% indicates that all available water is consumed and/or stored in the basin.

The second set of indicators focuses on the actual amount of water that is currently managed, or is available to be managed:

4. *Available Water (AW) = Gross inflow – Landscape Evapotranspiration - Reserved Flow* (km³/year), where landscape evapotranspiration is all water lost to evapotranspiration minus the evapotranspiration from managed land uses
   - Total amount of water that is available to be managed.

5. *Managed Water (MW) = Incremental ET of Managed Water Use* (km³/year)

6. *Managed Fraction = Managed Water / Available Water* (%)
   - Percentage of water that is actually managed from the total amount of water that is available.

Table 10: Data and calculation approach used for fluxes in WA+ Sheet 1. N/A stands for Not Available

WA+ Sheet 1 Flux	Description	Data used	Calculation approach
$P_{advection}$	Precipitation	WaPOR's L1_PCP_M	Aggregate by hydrological year
Q_{desal}	The inflow from desalinated water	N/A	-
Q_{sw}^{in}	The inflow from surface water (i.e. inter-basin surface water inflow)	N/A	-
Q_{gw}^{in}	The inflow from groundwater (i.e. interbasin groundwater inflow)	N/A	-
Gross Inflow	Total inflow from all sources	-	$P_{advection} + Q_{desal} + Q_{sw}in + Q_{gw}^{in}$
Net Inflow	The gross inflow and the storage change	-	Consumed water + Outflow
ΔS	Change in total water storage	-	Net Inflow – Gross Inflow
Rainfall ET PLU ULU MLU MWU	ET that occurs from effective rainfall and canopy interception. Effective rainfall is the part of the rain water that does not percolate below the root zone, flows away over the soil surface as run-off, or evaporates from canopy interception, thus, available in the root zone and can be used by the plants.	WaPOR-derived ET rainfall; WA+ Landuse maps	Aggregate by hydrological year and LU classes
Incremental ET PLU ULU MLU MWU	ET that occurs from other sources except effective rainfall and interception. For example, evaporation of irrigation water, evaporation of groundwater through deep rooted vegetation, water evaporation from a lake or other water surface that exceeds the rainfall on the water body itself.	WaPOR-derived ET incremental; WA+ Landuse maps	Aggregate by hydrological year and LU classes
Landscape ET	ET that occurs naturally, not due to water management (i.e. evaporation on managed reservoirs, or ET from irrigation water).	-	Rainfall ET + Total Incremental ET of PLU, ULU, MLU
Consumed water/ ET	ET occurs as interception, evaporation, soil evaporation, water evaporation, canopy transpiration/ The total Evapotranspiration is evapotranspiration from non-manageable, manageable and managed land uses.	WaPOR's L2_AETI_M	Aggregate by hydrological year
Utilized flow	ET from managed water use (i.e. irrigated crops, managed reservoirs)	-	MWU Incremental ET
Exploitable water	The net inflow minus Landscape ET	-	Utilized flow + Outflow
Q_{sw}^{outlet}	The river outflow at the outlet of the basin	Outflow estimated from literature	Aggregate by hydrological year
Q_{sw}^{out}	The outflow as surface water (i.e. interbasin surface water outflow)	N/A	-
Q_{gw}^{out}	The outflow as groundwater (i.e. interbasin groundwater outflow)	N/A	-
Non-consumed water /Outflow	Total outflow	-	$Q_{sw}^{outlet} + Q_{sw}^{out} + Q_{gw}^{out}$

3. Water Accounting Plus

3.1. The resource base

Table 10 provides description of the fluxes, the data sources and the calculation method used to produce sheet 1, the resource base.

3.1.1. Overview: Average over the entire period

The summary of average situation of the water resources in the Nile River Basin for the period from 2010 to 2018 is given in the WA+ sheet 1 as shown in Figure 17. The WA+ sheet 1 for individual years are provided in Annex 8. The year 2009 is considered as a 'warm-up' period for the pixel-based soil moisture balance model and therefore it is not included in the analyses.

The nine year average gross inflow is 2,085.9 km³/year while the total outflow from the basin is 2,163.8 km³/year with the difference 77.9 km³/year is supplied by depleting the storage. The exploitable water resources in the River Basin is 83.9 km³/year. The depletion in storage is contrary to the result obtained from GRACE which shows an increasing trend.

The highest water consumption is from the Utilized Land Use (1,027.2 km³/year from ET_{rain} and 426.7 km³/year from ET_{incr}). The Protected Land Use consumes the least water (98.1 km³/year from ET_{rain} and 24.9 km³/year from ET_{incr}). The Managed Water Use consumption is 164.4 km³/year (85.3 km³/year from ET_{rain} and 79.1 km³/year from ET_{incr}). The Modified Land Use category consumes about 417.7 km³/year with about 30% from ET_{rain}. The total ET_{incr} of the basin is about 30% of the gross inflow where about 12% of it is supplied from storage.

The majority (88%) of ET_{incr} (total volume 653.7 km³/year) originates from natural withdrawals (574.6 km³/year). The anthropic withdrawals (79.1 km³/year) is only is about 12% of ET_{incr}. The majority of the available water resources goes to Utilized Land Use (ULU) with 426.7 km³/year and Modified Land Use (MLU) with 123.1 km³/year. Protected Land Use (PLU) uses only 24.9 km³/year or less than 4% of the total ET_{incr}. Rarely this usage of blue water appears in water allocation plans, because this consumption occurs naturally and is out of sight from water managers. The fact that natural land use classes utilize blue water can be explained by capillary rise and flood plains flooded by overflows and from flash flood. Groundwater dependent ecosystems such as bushland and forests would tap into shallow aquifers and intercept drainage flows.

The total consumed water (the sum of rainfall and incremental ET) is 2,159 km³/year which is about 4% higher than the P. ET_{incr} accounts 30.3 % of the consumption.

Irrigated cropland covers 66,588 km² which is about 2% of the Nile River Basin area, this is about 10% lower than the 73,000 km³ as reported in the FAO Nile Basin information products (FAO, 2011). The average ET_{incr} used by this land cover is 894 mm/year (see Figure 16) which implies about 59.53 km³/year of the exploitable water or about 71% is used for irrigation. Of the managed water use the irrigated croplands consume about 75%.

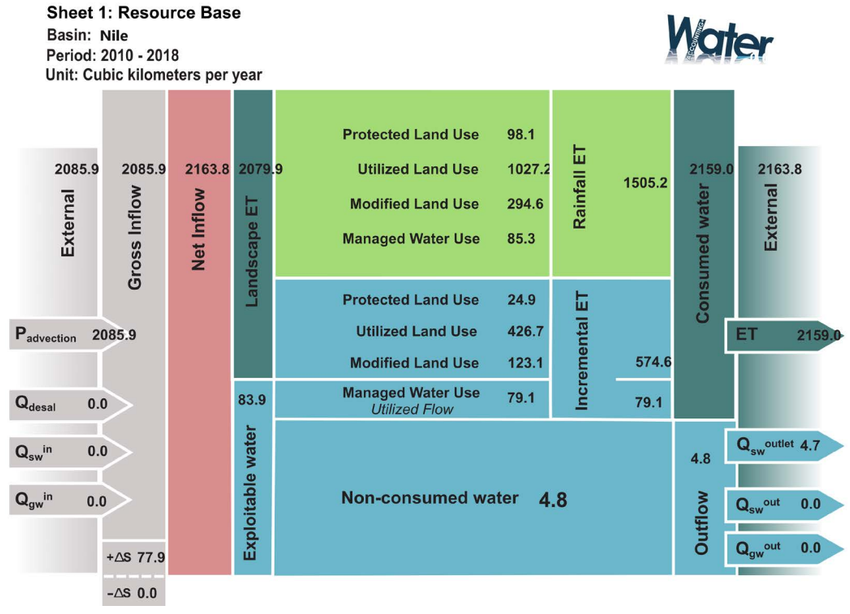

Figure 17: WA+ sheet 1 for the Awash River Basin containing average flow values for the period 2010 – 2018. Yearly Resource Base Sheets are included in Annex 8

The water resources situation described above shows the average condition over nine years from 2010 to 2018, however to understand the variation from year to year in relation to precipitation the basin receives, the yearly situation of the water resources is described in the following section.

3.1.2. Variability of the annual Water Accounts

Figure 18 shows the yearly changes in precipitation, ET_a and ET_{rain} and ET_{incr} per WA+ land use categories. It shows that ET_{rain} follows the same trend as precipitation except for the year 2012 which is the wet year in the studied period. In this year the ET_{rain} didn't increase with the precipitation. ET_{incr} shows opposite trend with the precipitation. ET_{incr} seem decreasing when precipitation is increasing and increasing as P decreases. This maybe indicate that part of the ET_{incr} is supplied from groundwater sources or uncertainty associated with WaPOR P and ET_a. This may also explain the fact that ET is greater than precipitation in almost all the years except the wet year (2012). Since reliable source of ground water abstraction was not found, any consumption from the groundwater was not included in the water account study.

The year 2012, the wettest year from the period analysed, received 2,225.6 km³ or 710 mm/year of rainfall (Figure 19). The exploitable water resources is 154.4 km³/year which is very different from that of the average situation. The main difference is in the amount of water stored in the basin which now increased to 71.7 km³/year. The proportion of ET_{rain} and ET_{incr} more or less remained the same.

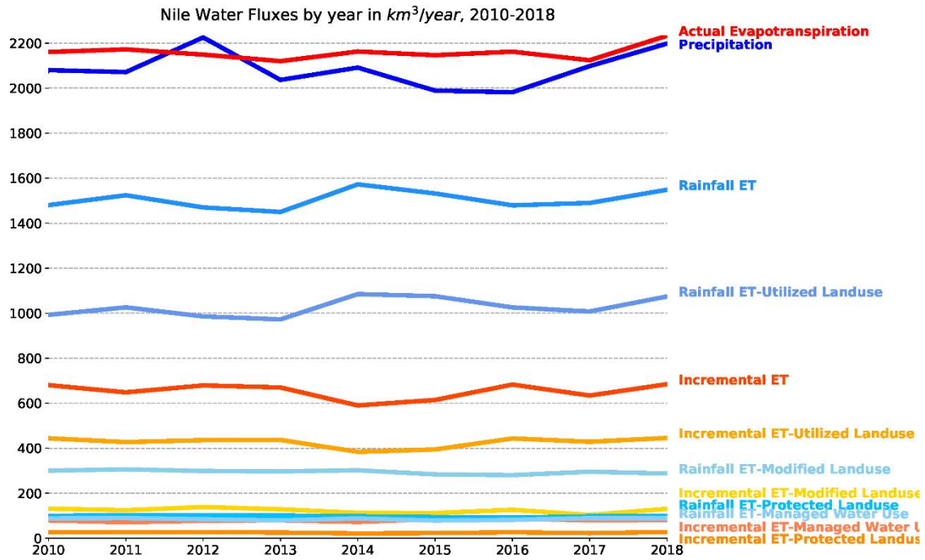

Figure 18: Nile River Basin water fluxes by year from 2009 to 2018

ET_{incr} shows a reduction (13.4 km³/year) as part of it was satisfied by rainfall. The total consumption is 65.3 km³/year which accounts 79% of the precipitation the basin received. ET_{incr} is only 20% of the total consumption.

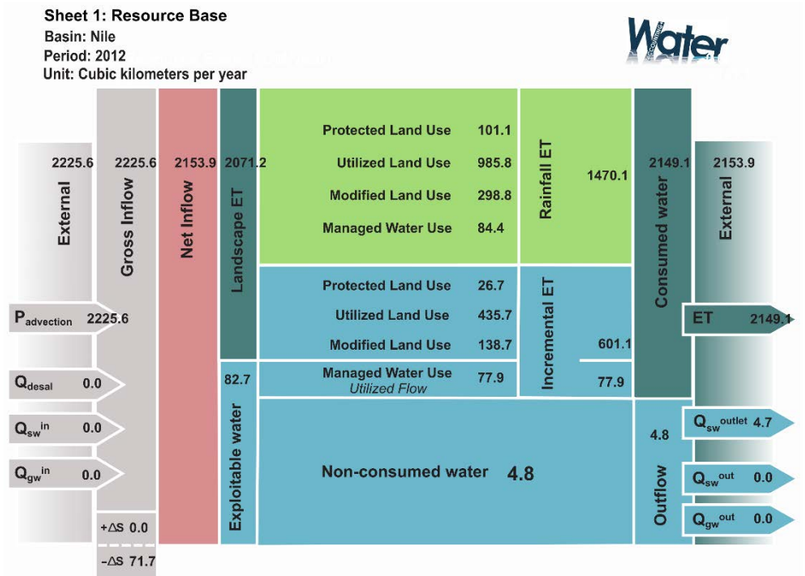

Figure 19: WA+ sheet 1 for the Nile River Basin for the wettest year (2012)

On the other hand, 2016 was the driest year receiving just 1,981.9 km³/year or 633 mm/year which is less than the consumed water (by 180.3 km³/year), the difference supplied from depleting the storage in the basin. ET_{incr} (185.1 km³/year) is now 9% of the total consumed water (Figure 20).

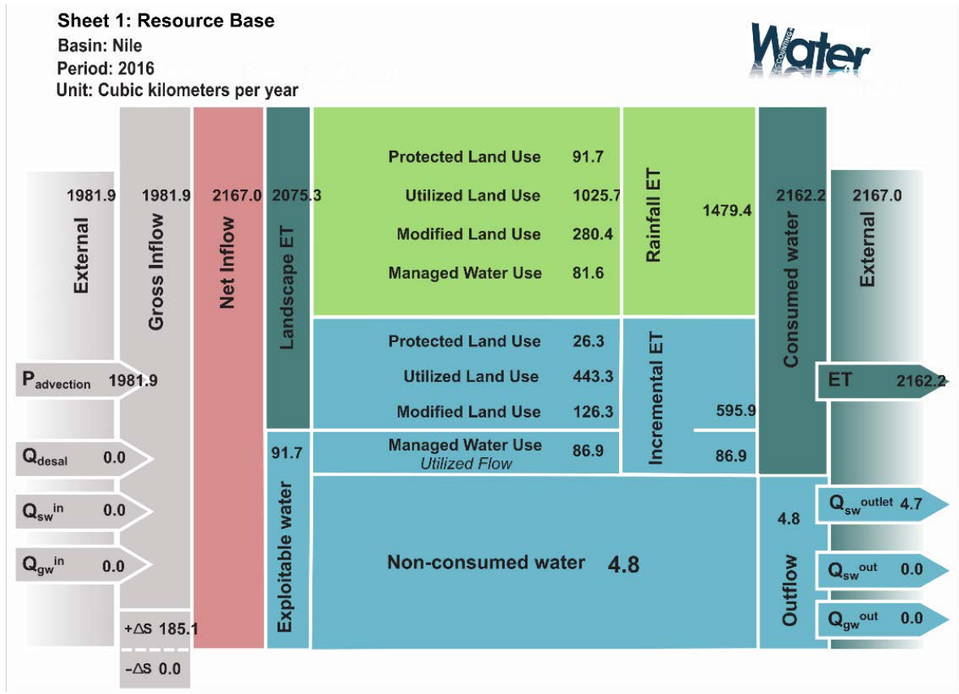

Figure 20: WA+ sheet 1 for the Nile River Basin for the driest year (2016)

3.2. Key Indicators

The key performance indicators are presented in Table 11. Since there were discrepancies between the storage change computed from WaPOR data, GRACE gravity measurements, and change in storage computed from yearly water balance (Table 3), the later was used for computation of the key indicators as shown in Table 11. The average ET fraction of the basin is 107.4 indicating consumption more than the average precipitation by about 7.4%. This difference is supplied from depletion of storage. However, GRACE total storage change estimates an increase in storage. Because of this discrepancy, the state of total water storage change from 2010-2018 cannot be reliably estimated.

Table 11: WA+ Sheet 1 key indicators of Awash River Basin from 2010 to 2018 based on water balance derived from WaPOR datasets

Year	ET fraction (%)	Stationarity index (%)	Basin Closure (%)	Available water (km³/year)	Managed water (km³/year)	Managed fraction (%)
2010	103.9	-4.0	99.8	-1.6	79.0	-4,967.0
2011	104.9	-4.9	99.8	-30.0	70.8	-235.8
2012	96.6	3.3	99.8	154.4	77.9	50.5
2013	104.1	-4.2	99.8	-3.9	79.3	-2,009.8
2014	103.4	-3.5	99.8	1.2	72.4	6,235.8
2015	107.9	-7.6	99.8	-72.2	85.2	-118.0
2016	109.1	-8.6	99.8	-93.4	86.9	-93.0
2017	101.2	-1.4	99.8	53.8	79.6	147.9
2018	101.6	-1.8	99.8	45.9	80.7	175.8
Average	107.4	-6.4	99.8	-55.9	78.7	-152.0

3.2.1. ET fraction, Stationarity index and Basin Closure

The key performance parameters presented in Table 11 describes the river basin system by a few indicators. The ET fraction is highest in 2016 with about 109.1% indicating more than the precipitation amount was consumed in that year. The additional amount consumed (9%) comes from storages in the basin. The ET fraction is lowest for the year 2012 with 96.6% indicating that not all rainfall is consumed so that surplus of rainfall is used to increase storage in the basin. The representative value for ET fraction across the study period (2009 to 2010) is 107.4%. On average the basin consumes more than the precipitation it receives.

The Stationarity Index indicator describes what percentage of the consumption is originating from storage changes. An average positive indicator of -6.49% means that wither groundwater or storage in the reservoirs were being exploited and there was no net recharge in the period studied. The only year from 2010 to 2018 when the groundwater was recharging and/or storage in the basin was increasing marginally was 2012.

The average basin closure index is 99.8%, which shows that all water resources is consumed and/or stored in the basin.

3.2.2. Available water, managed water and managed fraction

The second set of indicators in Table 11 focuses on the actual amount of water that is currently managed, or is available to be managed. The total amount of Available Water is -55.9 km³/year depicting a situation where more water than the available is already managed. 55.9 km³/year is being managed in addition to the average 78.7 km³/year. The withdrawal is much more that the safe cap of water withdrawals, therefore, it is essential that further withdrawals should be compensated by equivalent reduction of consumptions through improving water productivity.

In the only wet year the available water increases and the managed fraction becomes less while in the rest of the studied period (dry years) the available water was less that the managed and the managed fraction increase. A negative managed fraction indicates that the managed water provided by depleting storage in the basin.

During period when there would be surplus available water, part of it can be contaminated by anthropogenic pollution loads to the extent that exceeds the basin's assimilation capacity. The water pollution level of the Nile River Basin related to anthropogenic Nitrogen and Phosphorus loads from diffuse and point sources from 2002 to 2010 was estimated to be less than 0.5 (Mekonnen and Hoekstra, 2015) and between 2 and 5 (Mekonnen and Hoekstra, 2018) respectively. In these studies, the water pollution levels were calculated as the ratio of Grey Water Footprint over the annual actual runoff of the basin. These values indicate that it would take more than 2 to 5 times of actual runoff of the basin to dilute the pollution related to anthropogenic Nitrogen and Phosphorus loads. As a result, any available water might not be suitable for some uses (irrigation, drinking water, etc.). It should be, however, noted that the uncertainty range of the global GWF is of -33% to +60% (Mekonnen and Hoekstra, 2015).

4. Conclusions

The Nile River Basin faces a huge challenge in terms of water security. With an expected doubling of the population in the basin in the next twenty five years, water supply in the basin will further be depleted as demands for agriculture, domestic and industry continues to grow. Water resources of the basin are already being intensively utilised and as such the basin is considered as the one of the conflict-prone river basins. Hence, assessing the state of water resources in the basin can provide invaluable information for stakeholders and decision maker for collaborative and sustainable development of the basin and beyond.

A simple and rapid water accounting of the Nile River Basin has been performed using mainly the FAO WaPOR database for the period 2009 to 2018. The study revealed that for the period 2019 to 2018 the evapotranspiration (ET_a) is greater than the precipitation (P) except for year 2012. Even with a very small proportion (0.23%) of outflow from the average gross inflow to the basin, part of the consumption is supplied by depleting water from the storage in the basin.

The spatial patterns of the difference between P and ET_a revealed that ET_a far exceeds P in water bodies in the Sudan and Egypt such as in the Sudd wetlands, in Aswan reservoir and irrigated farmlands along the banks of the river in Egypt whereas P exceeds ET_a in the Ethiopian highlands and the Equatorial Plato.

The WaPOR 2.0 Level 2 data quality assessments showed reasonable estimates of P and ET_a at basin scale and as such can be useful to map the general spatial distribution and identify areas of net water generation and water consumption in the basin. However, the water consumption in bare and sparse land use is unrealistic and could be due to uncertainties in P and/or ET_a.

Irrigated croplands consume far greater amount of water than precipitation but these are not the only consumer land use cover types. Natural land covers also consumed water though in a lesser degree. Land cover in the basin remains largely unchanged though out the decade, except small percentage change of irrigated cropland to rainfed cropland and vice versa, and as such the water consumption pattern remained the same.

The average WaPOR based gross inflow (2,086 km³/year) is less than the total outflow (2,164 km³/year) with the difference being (77.9 km³/year) indicating there is no outflow from the basin. There is huge uncertainty associated with the values of P and ET_a, for example, the consumption of blue water by natural land covers such as grassland, shrub lands and bare or sparse vegetation, which is more than 90 km³/year, is more than the difference between gross inflow and total out flow. If the data is corrected for this (no blue water consumption for these land cover types), the gap between inflow and outflow would be in the right order of magnitude compared to observed outflow.

It is clear from the analysis that even if the WaPOR P and ET_a have inherent errors especially for low values in the low lands and thus the water balance is not accurate, the basin is a closed basin in a way that the outflow is a very small fraction of the inflow and all the remaining water is consumed together with storage depletion. Therefore, the potential for agriculture expansion in the basin is almost none form water resources perspective, even though the irrigated land accounts only to two percent of the total area. The largest proportion of the water in the basin is consumed by natural land covers. The largest net water consumption is from bare/sparse vegetation cover. The beneficial water consumption contribution to ET_a is low compared to non-beneficial consumptions. Agricultural expansion in the basin can be implemented if non-consumptive use of water by natural land covers is minimized through improvement of landscape strategies. However, such expansion should take into account the impacts of land uses changes and its impact on hydrological response of the basin, environmental flow requirements, fair share of the water resources among the riparian countries and impacts of climate variability on seasonal and periodic availability of water resources.

References

Bastiaanssen, W.G.M., Karimi, P., Rebelo, L.-M., Duan, Z., Senay, G., Muthuwatte, L. & Smakhtin, V. 2014. Earth observation based assessment of the water production and water consumption of Nile Basin agro-ecosystems. *Remote Sensing,* 6, 1030610334. https://doi.org/10.3390/rs61110306

Biancamaria, S., Mballo, M., Le Moigne, P., Pérez, J.M.S., Espitalier-Noël, G., Grusson, Y., Cakir, R., Häfliger, V., Barathieu, F., Trasmonte, M. & Boone, A. 2019. Total water storage variability from GRACE mission and hydrological models for a 50,000 km² temperate watershed: the Garonne River basin (France). J*ournal of Hydrology: Regional Studies*, 24, p.100609.

Bouraoui, F., Grizzetti, B., & Aloe, A. 2010. Estimation of water fluxes into the Mediterranean Sea. *Journal of Geophysical Research: Atmospheres*, 115(D21).

de Boer, F. 2016. *HiHydroSoil: A High Resolution Soil Map of Hydraulic Properties* (Version 1.2).

Dost R., Obando E. B., Bastiaanssen W. & Hoogeveen J. 2013. *Water Accounting Plus (WA+) in the Awash River Basin.* A report submitted to FAO for the Coping with water scarcity – developing national water audits Africa project.

FAO. 2011. *Information Products for Nile Basin Water Resources Management*. Synthesis report. Rome

FAO. 2018. *WaPOR Database Methodology: Level 1.* Remote Sensing for Water Productivity Technical Report. Rome

FAO. 2019. *FAO Water Productivity - Catalog - Land Cover Classification.* https://wapor.apps.fao.org/catalog/2/L2_LCC_A (accessed 9.20.19).

FAO & IHE Delft. 2019. *WaPOR quality assessment.* Technical report on the data quality of the WaPOR FAO database version 1.0. Rome. 134 pp. Available at http://www.fao.org/3/ca4895en/CA4895EN.pdf

FAO & IHE Delft. 2020. *Water accounting in the Awash River Basin*. FAO WaPOR water accounting reports. Rome. 41 pages.

FAO & IHE Delft. 2020 a. *Rapid Water Accounting in the Jordan River Basin*. FAO WaPOR water accounting reports [in press].

FAO & IHE Delft. 2020 b. *Rapid Water Accounting in the Niger River Basin.* FAO WaPOR water accounting reports [in press].

Funk, C., Peterson, P., Landsfeld, M., Pedreros, D., Verdin, J., Shukla, S., Husak, G., Rowland, J., Harrison, L., Hoell, A. & Michaelsen, J. 2015. *The climate hazards infrared precipitation with stations — a new environmental record for monitoring extremes*. Scientific data, 2, 150066.

GRID-Arendal. 2019. *River discharge of freshwater into the Mediterranean*. URL http://www.grida.no/resources/5897 (accessed 9.20.19).

Hilhorst, B., Burke, J., Hoogeveen, J., Fremken, K., Faures, J.-M. & Gross, D. 2011. *Information Products for Nile Basin Water Resources Management*; FAO: Rome, Italy; p. 130.

Karimi, P. 2014. *Water Accounting Plus for Water Resources Reporting and River Basin Planning* (PhD thesis). TU Delft, Delft, The Netherlands.

Karimi, P. & Bastiaanssen, W.G.M. (2015). Spatial evapotranspiration, rainfall and land use data in water accounting - Part 1: Review of the accuracy of the remote sensing data. *Hydrological Earth Systems Science*, 19, 507–532. https://doi.org/10.5194/hess-19-507-2015

Lehner, B., C. Reidy Liermann, C. Revenga, C. Vorosmarty, B. Fekete, P. Crouzet, P. Doll, M. Endejan, K. Frenken, J. Magome, C. Nilsson, J.C. Robertson, R. Rodel, N. Sindorf, & D. Wisser. 2011. *Global Reservoir and Dam Database*, Version 1 (GRanDv1): Reservoirs, Revision 01. Palisades, NY: NASA Socioeconomic Data and Applications Center (SEDAC).https://doi.org/10.7927/H4HH6H08. Accessed 5 August 2019.

Lehner, B. & Grill G. 2013. Global river hydrography and network routing: baseline data and new approaches to study the world's large river systems. *Hydrological Processes*, 27(15): 2171–2186. Data is available at www.hydrosheds.org.

Luthcke, S.B., T.J. Sabaka, B.D. Loomis, A.A. Arendt, J.J. McCarthy & J. Camp. 2013. Antarctica, Greenland and Gulf of Alaska land ice evolution from an iterated GRACE global mascon solution, J. Glac., Vol. 59, No. 216, 613-631, doi:10.3189/2013JoG12J147.

MacAlister, C.; Pavelic, P.; Tindimugaya, C.; Ayenew, T.; Ibrahim, M. E. & Meguid, M. A. 2012. *Overview of groundwater in the Nile River Basin.* In Awulachew, S.B; Smakhtin, V., Molden, D., Peden D. (Eds.). The Nile River Basin: water, agriculture, governance and livelihoods. Abingdon, UK: Routledge. pp. 186-211.

Mekonnen, M.M. & Hoekstra, A.Y. 2015. Global Gray Water Footprint and Water Pollution Levels Related to Anthropogenic Nitrogen Loads to Fresh Water. *Environmental Science & Technology,* 49, 12860–12868. https://doi.org/10.1021/acs.est.5b03191

Mekonnen, M.M. & Hoekstra, A.Y. 2018. Global Anthropogenic Phosphorus Loads to Freshwater and Associated Grey Water Footprints and Water Pollution Levels: A High-Resolution Global Study. *Water Resources Research,* 54, 345–358. https://doi.org/10.1002/2017WR020448

Molden, D. 1997. Accounting for Water Use and Productivity. Swim paper. Colombo, Sri Lanka. Retrieved from http://www.iwmi.cgiar.org/Publications/SWIM_Papers/PDFs/SWIM01.PDF

NBI. 2017. *Nile Basin Water Resources Atlas.* URL: http://atlas.nilebasin.org (accessed 9.16.19).

Nile Waters. 2014. *Understanding the Nile Basin Hydrology; Mapping Actual Evapotranspiration Over the Nile Basin*. Technical Bulletin from The Nile Basin Initiative Secretariat Issue: 01 Year: 2014

UNEP-WCMC. 2019. *User Manual for the World Database on Protected Areas and world database on other effective area-based conservation measures*: 1.6. Cambridge, UK. Available at: http://wcmc.io/WDPA_Manual

Yang, Y., Donohue, R.J. & McVicar, T.R. 2016. Global estimation of effective plant rooting depth: Implications for hydrological modeling. *Water Resources Research*. 52, 8260–8276. https://doi.org/10.1002/2016WR019392

Appendixes

Annex 1 Plots of Annual Precipitation of Nile River Basin in mm/year

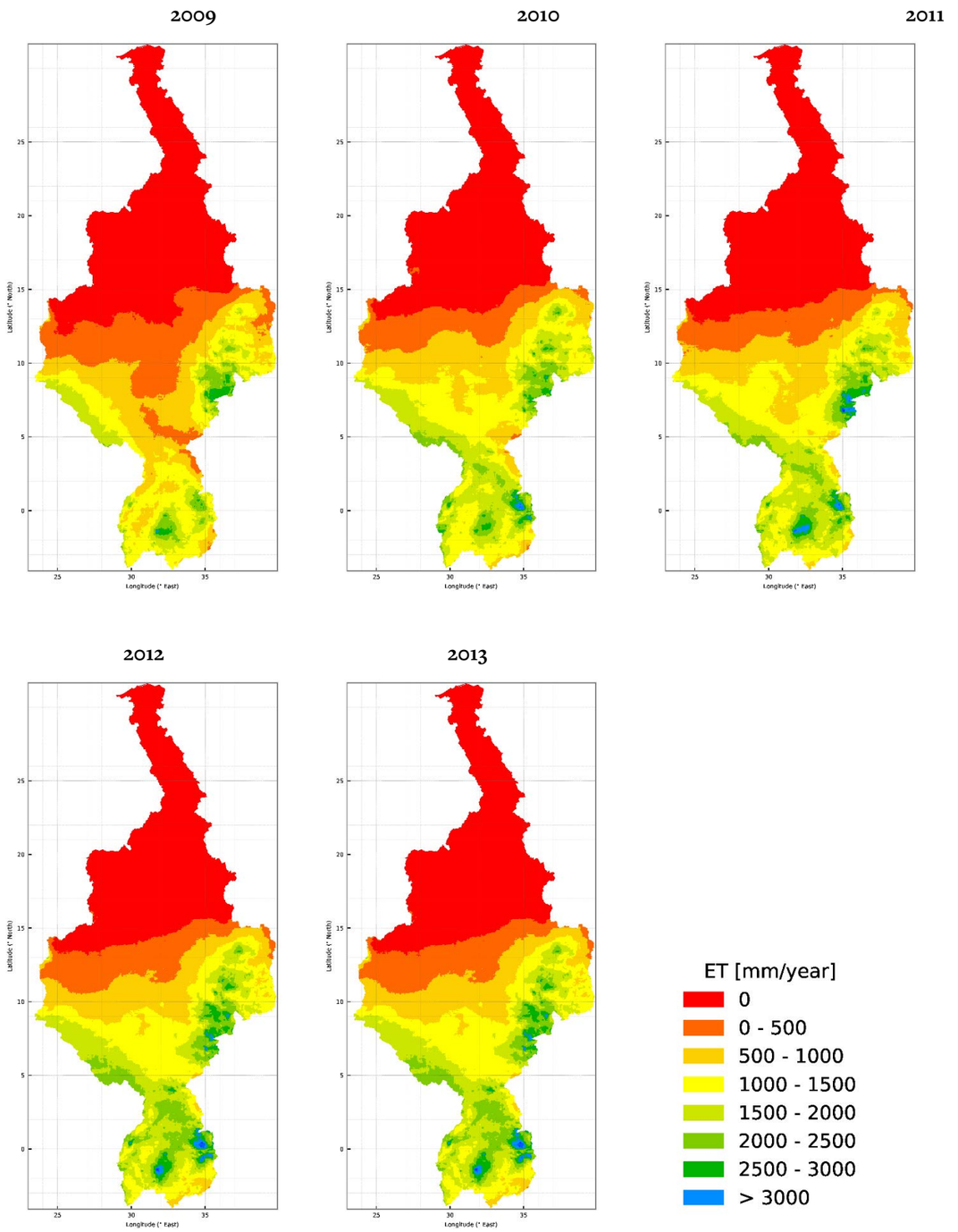

Annex 2 Plots of Annual Actual Evapotranspiration of Nile River Basin in mm/year

2009

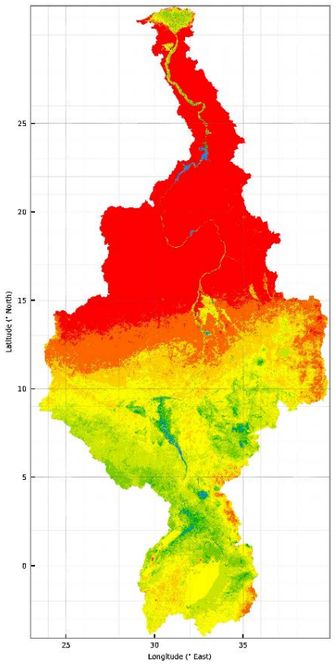

2010

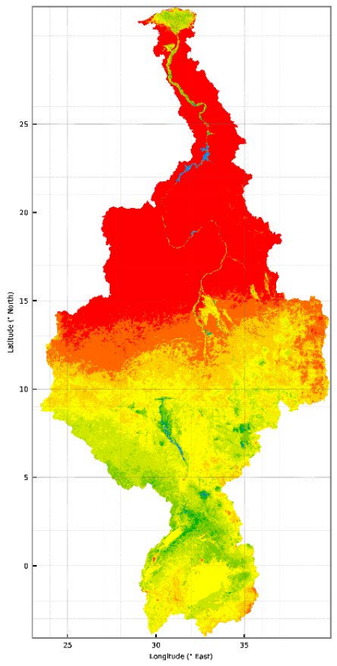

2011

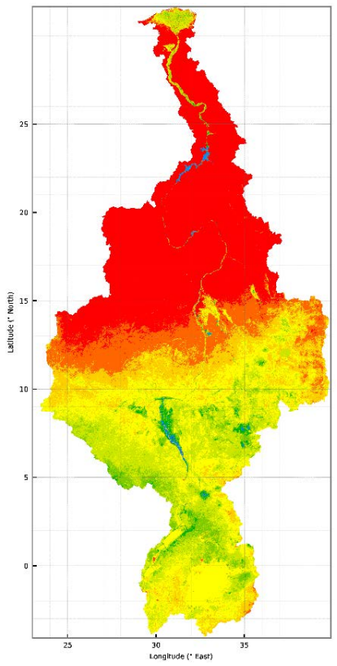

2012

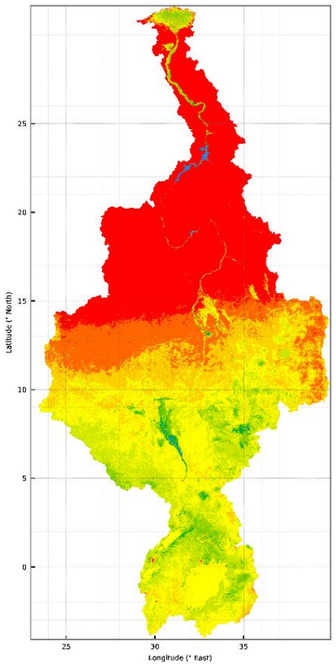

2013

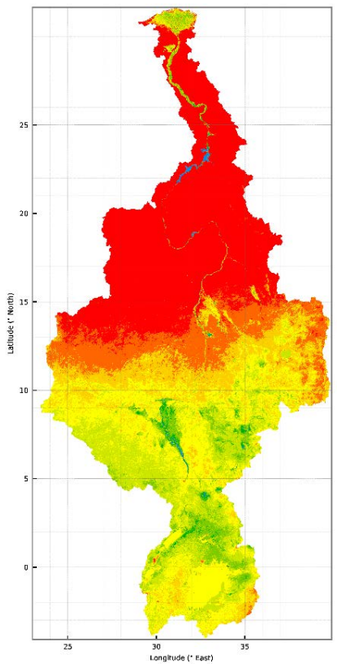

ET [mm/year]
0
0 - 500
500 - 1000
1000 - 1500
1500 - 2000
2000 - 2500
2500 - 3000
> 3000

2014

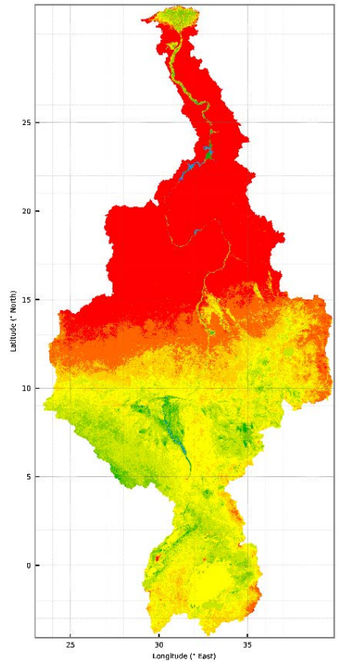

2015

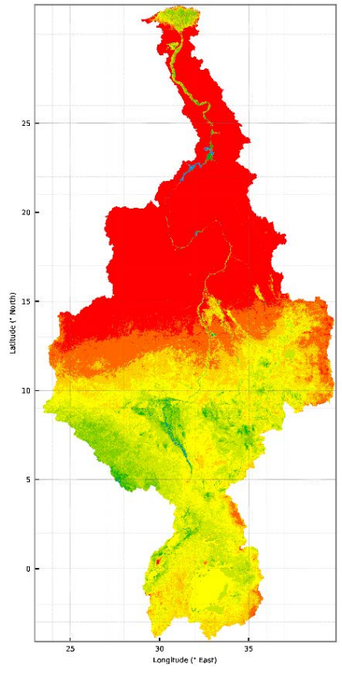

2016

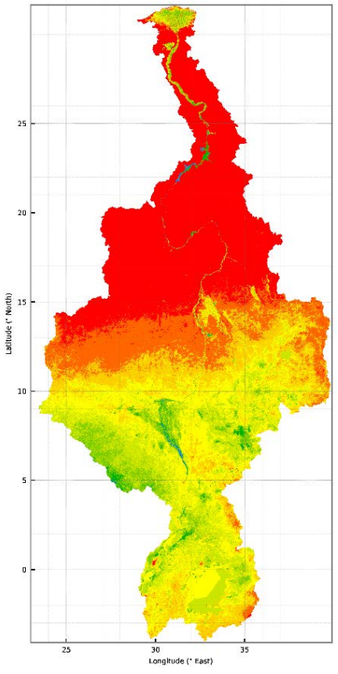

2017

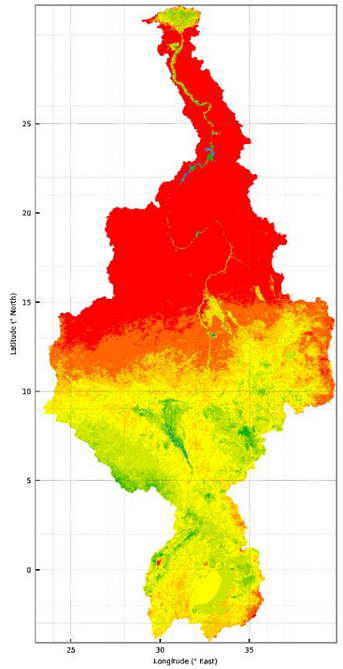

2018

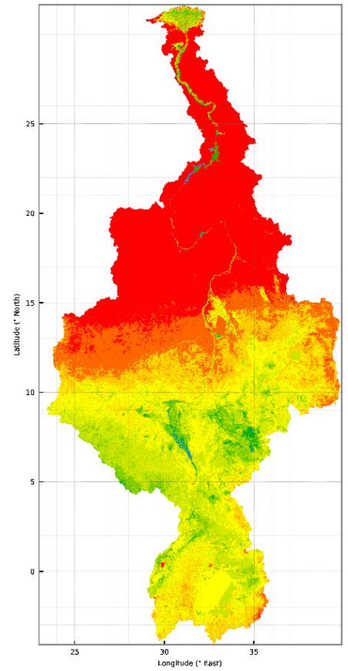

ET [mm/year]
0
0 - 500
500 - 1000
1000 - 1500
1500 - 2000
2000 - 2500
2500 - 3000
> 3000

Annex 3 Plots of Annual P – ET_a of Nile River Basin in mm/year

2009

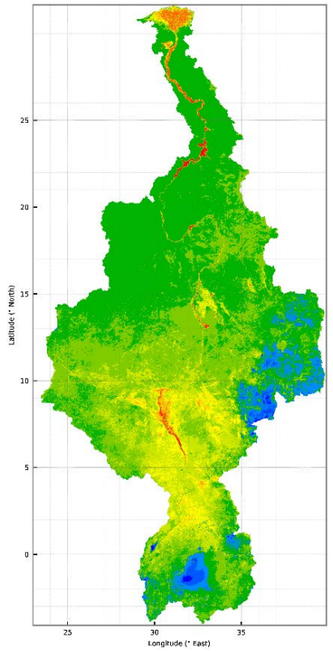

2010

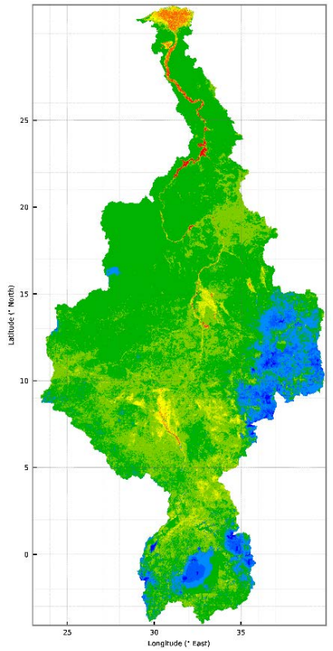

2011

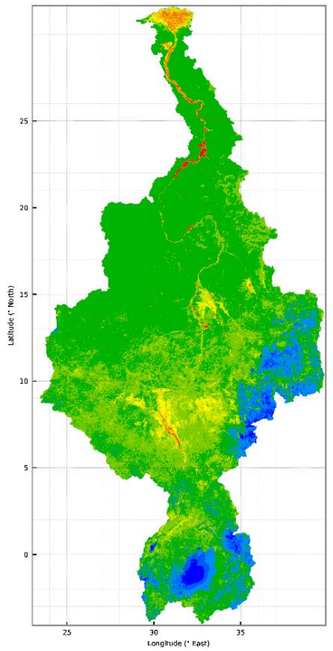

2012

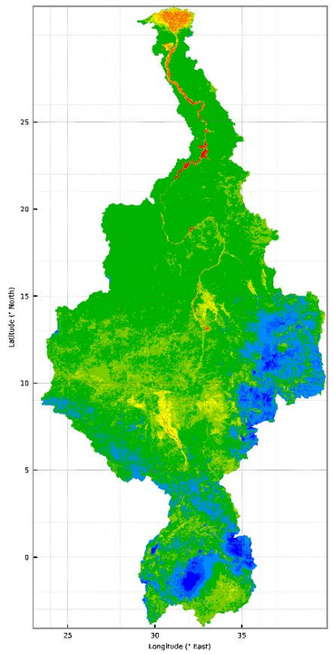

2013

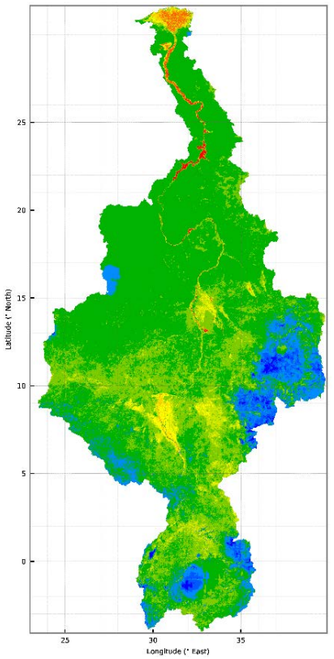

P-ET [mm/year]

- < -2000
- -2000 - -1600
- -1600 - -1200
- -1200 - -800
- -800 - -400
- -400 - 0
- 0 - 400
- 400 - 800
- 800 - 1200
- > 1200

2014

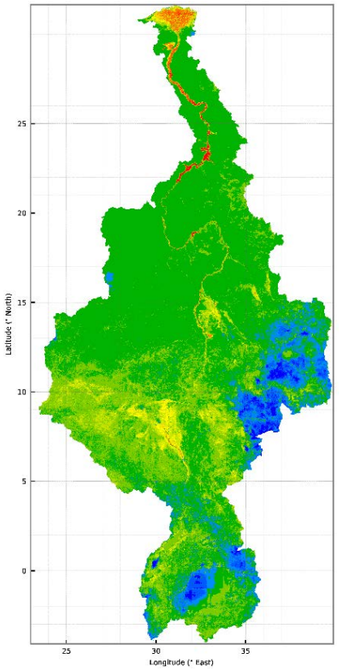

2015

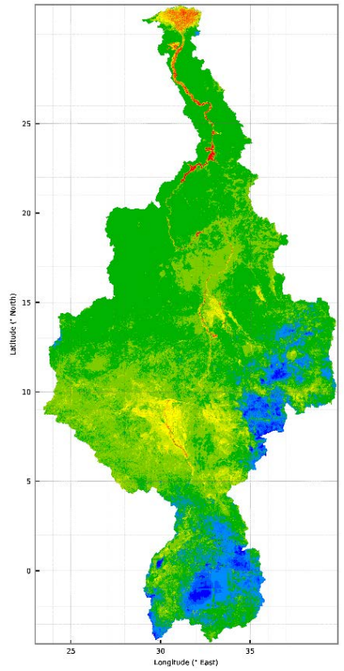

2016

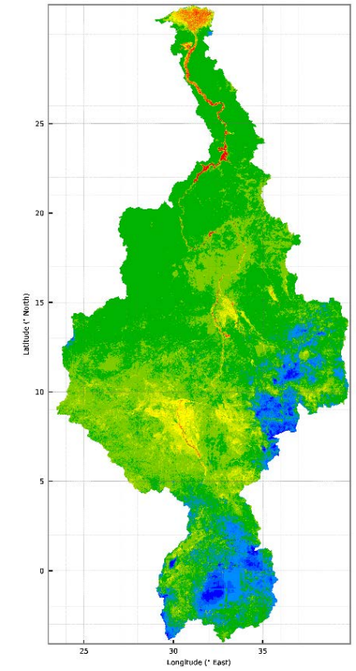

2017

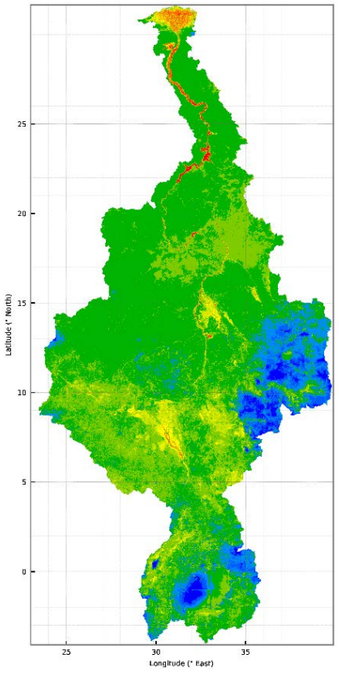

2018

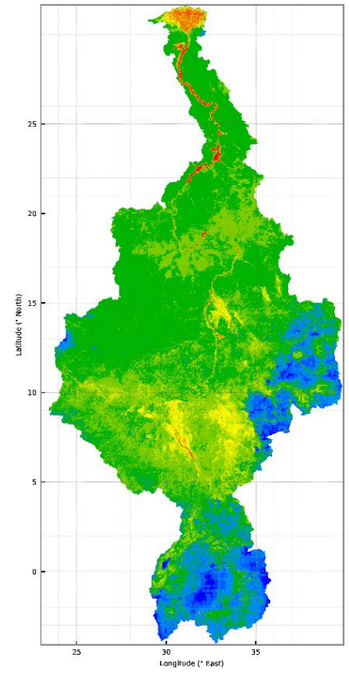

P-ET [mm/year]

- < -2000
- -2000 - -1600
- -1600 - -1200
- -1200 - -800
- -800 - -400
- -400 - 0
- 0 - 400
- 400 - 800
- 800 - 1200
- > 1200

Annex 4 Plots of Annual Land cover classification maps

2009

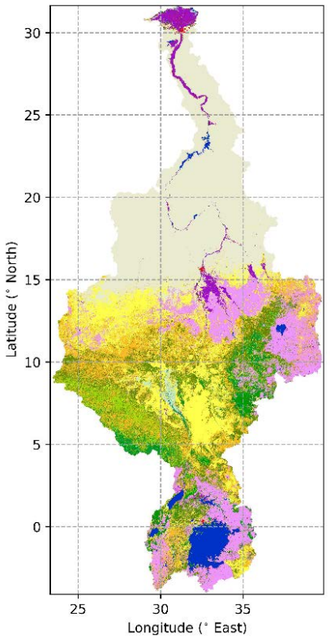

2010

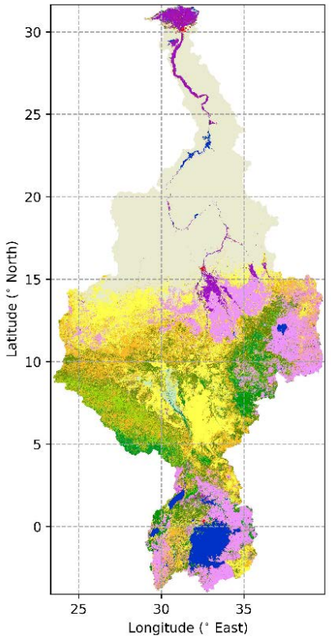

2011

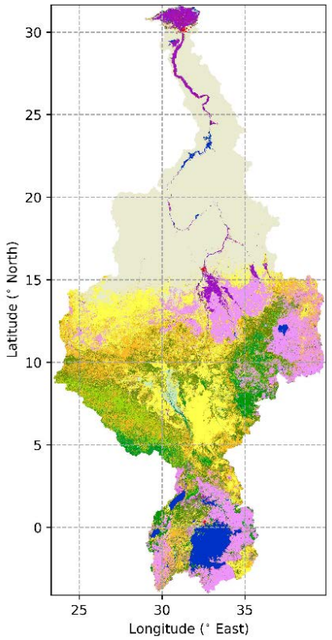

2012

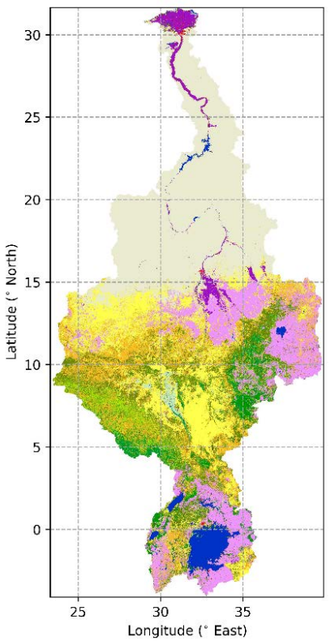

2013

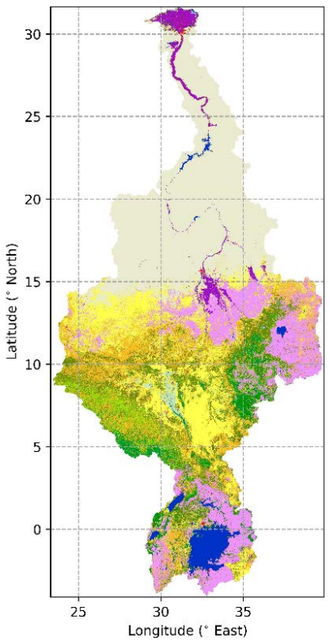

2014

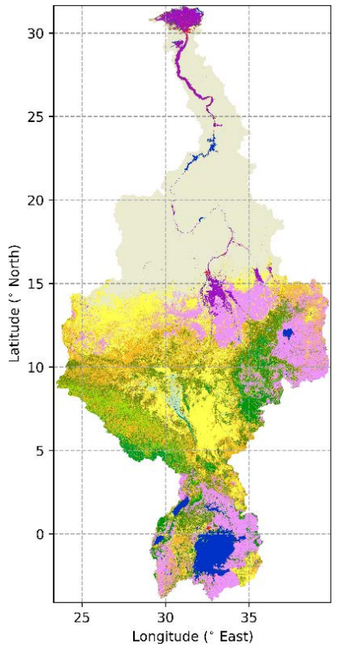

2015

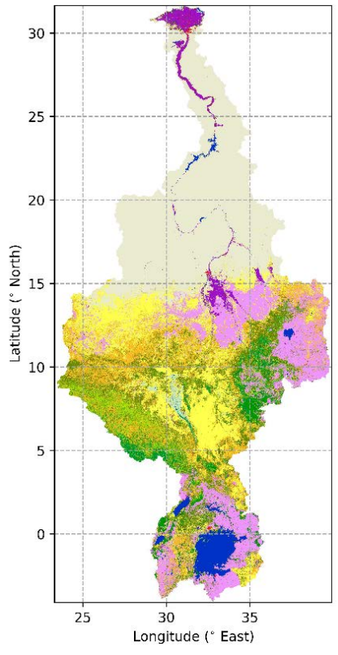

2016

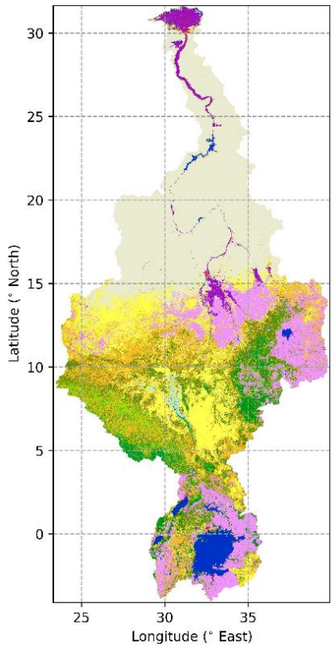

2017

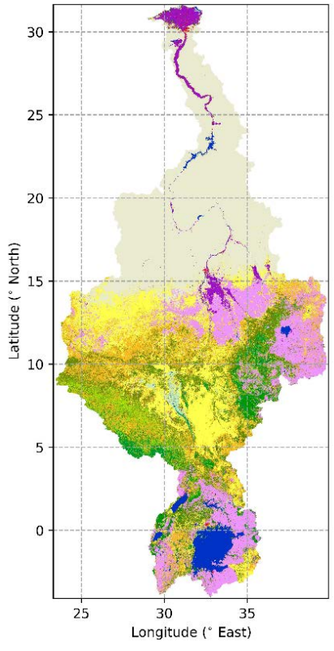

2018

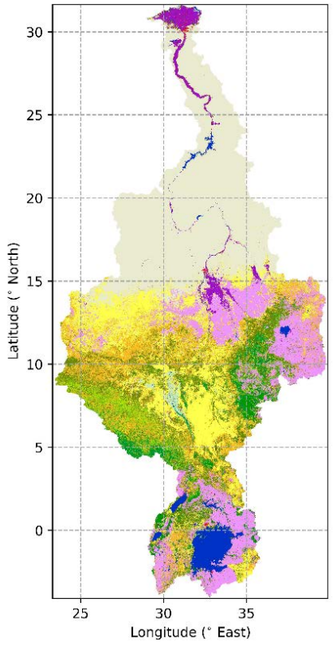

Annex 5 Plots of Annual Land Use maps based on WA+ Categories

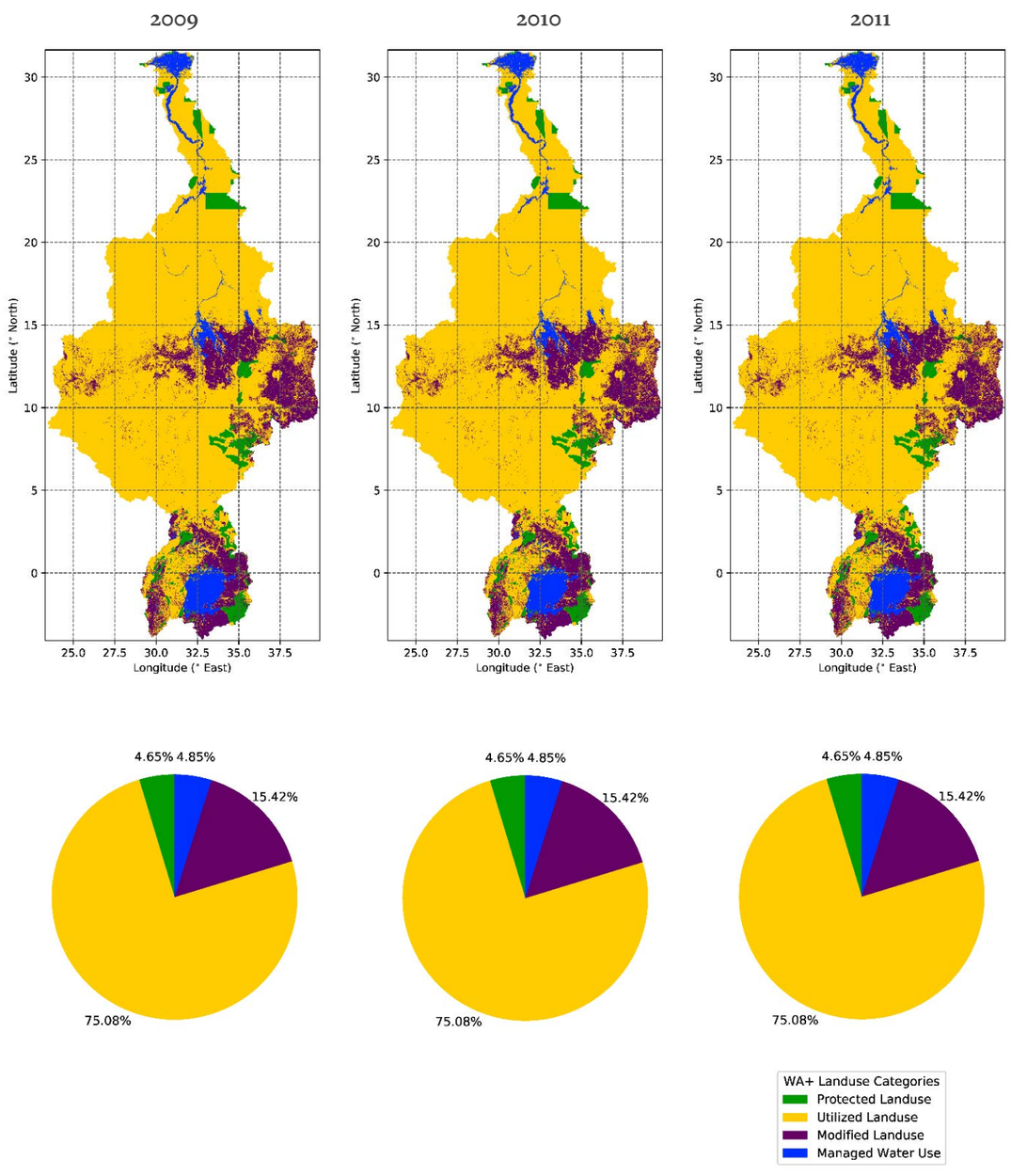

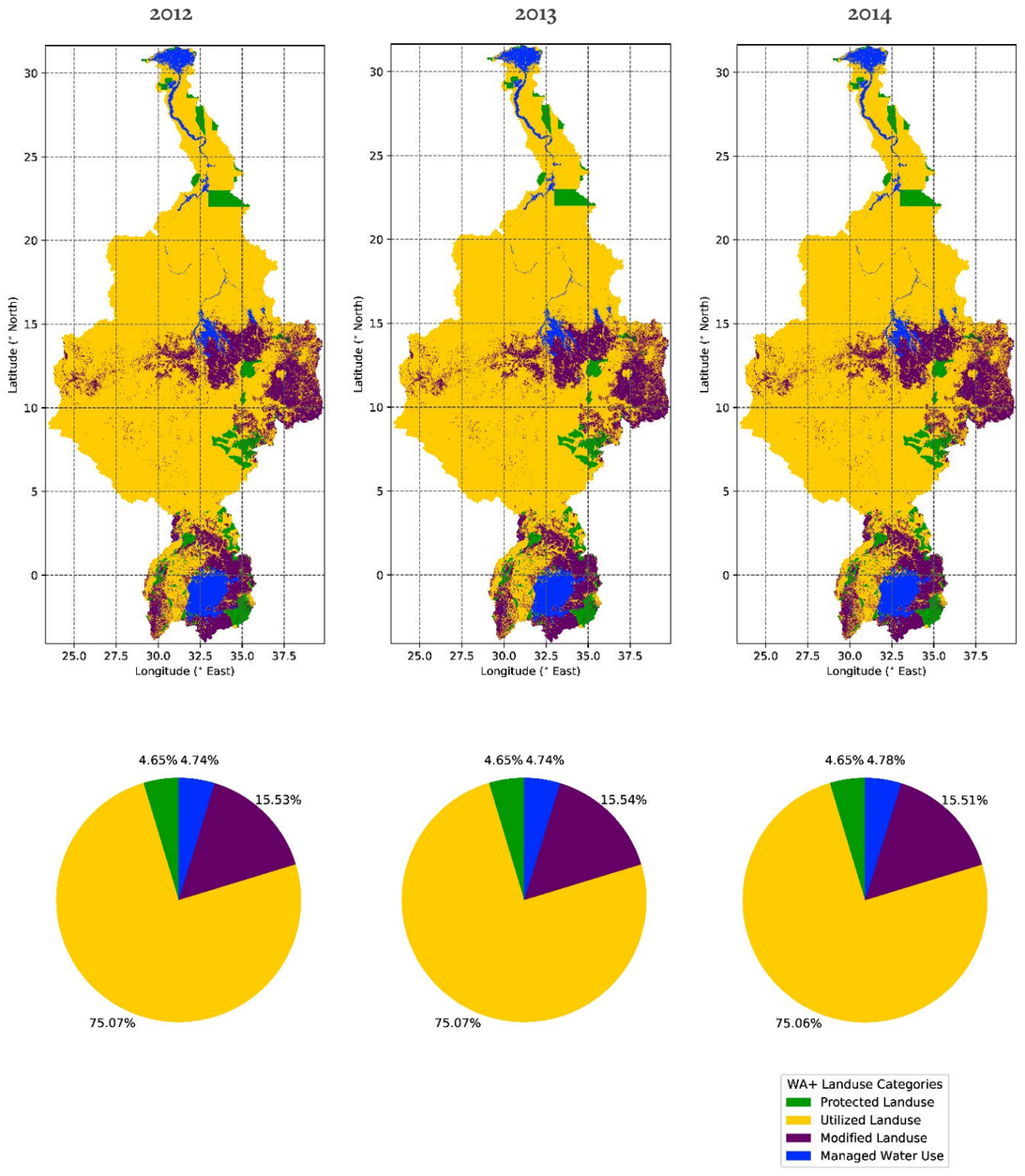

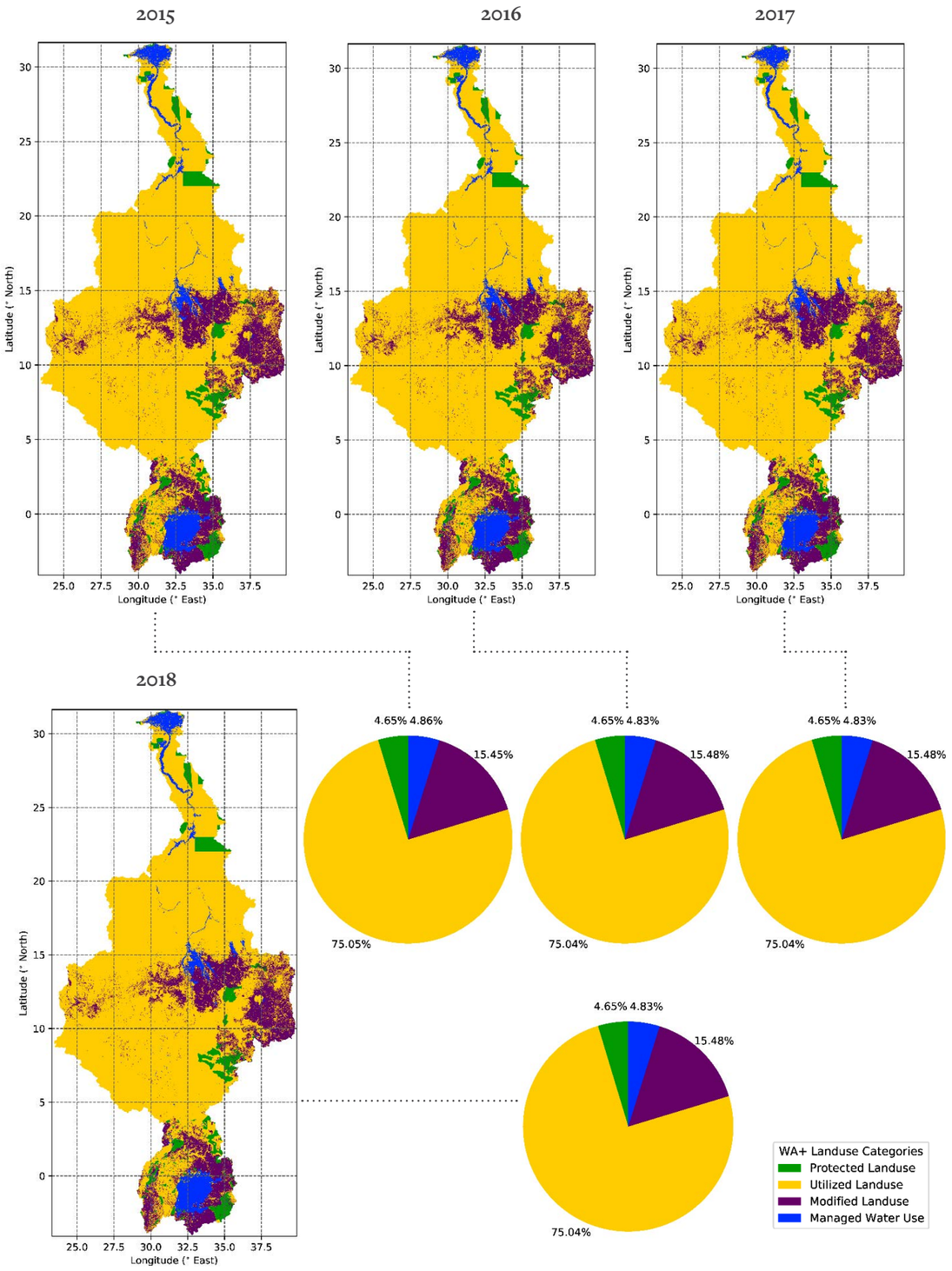

Annex 6 Annual estimated Incremental ET (ET_{incr}) of individual years

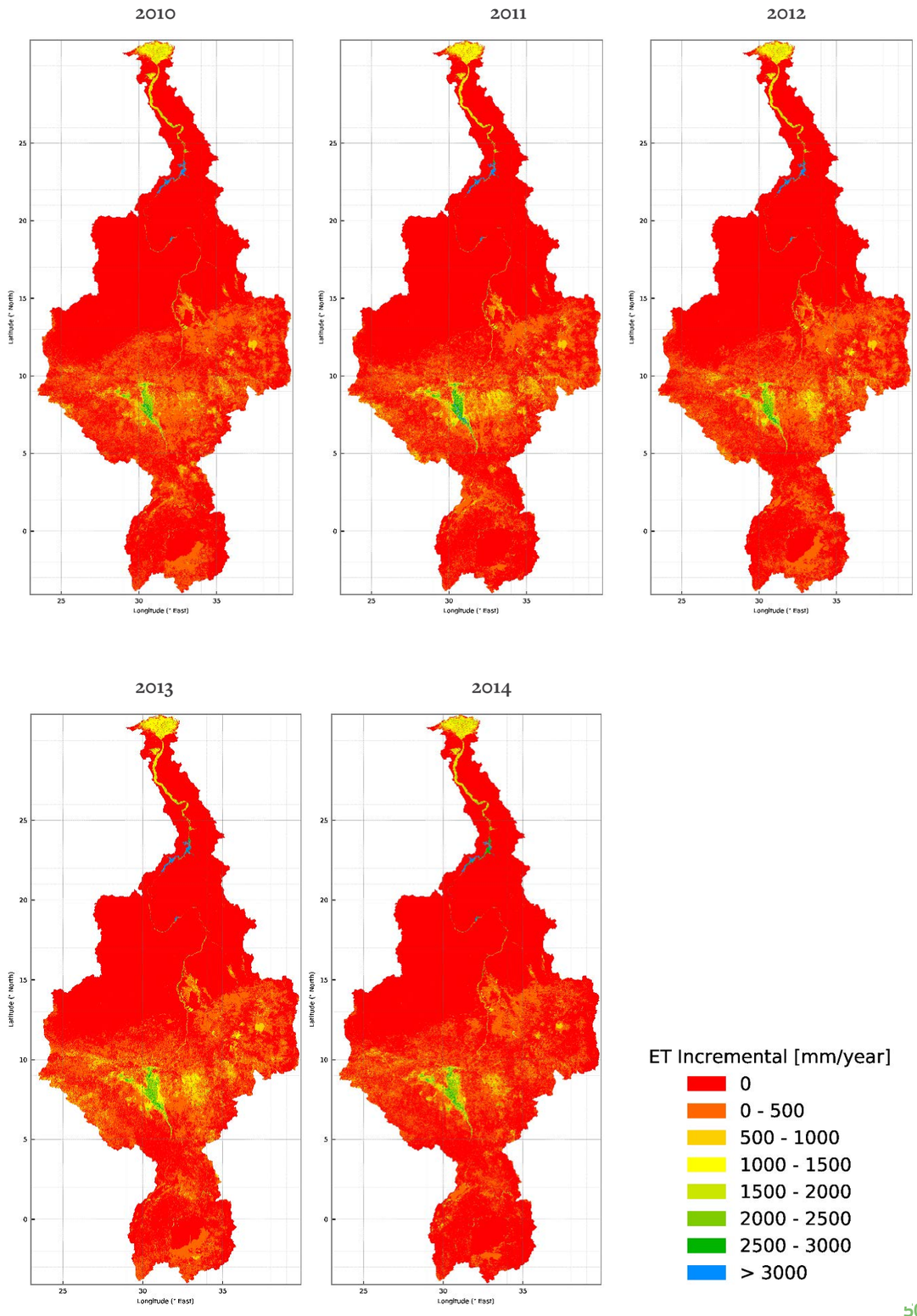

2015

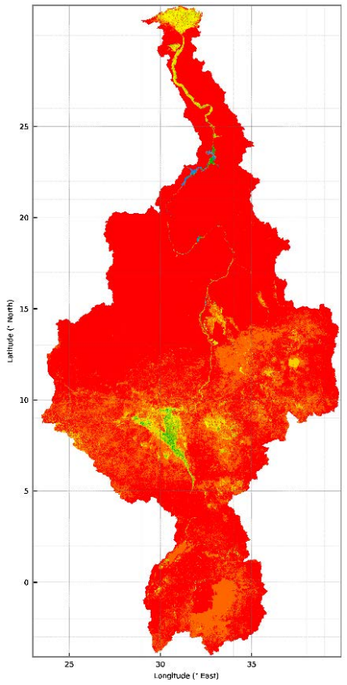

2016

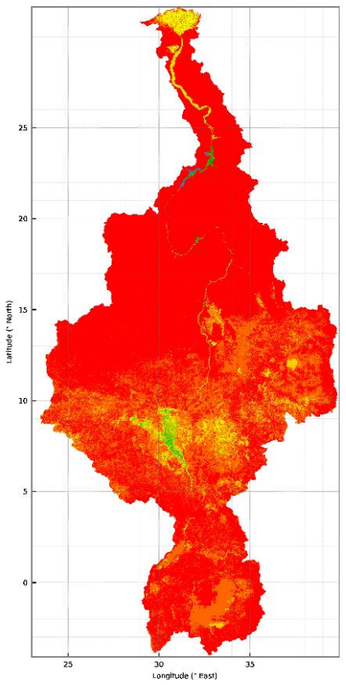

2017

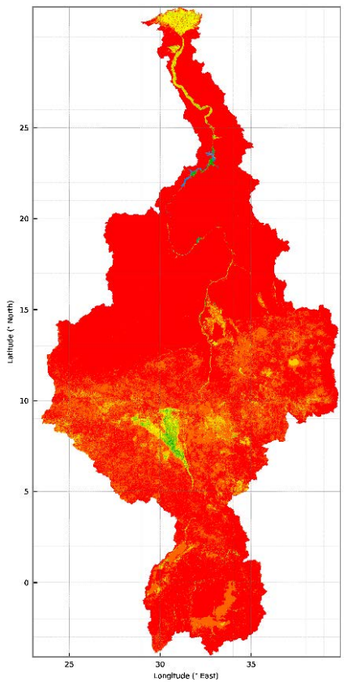

2018

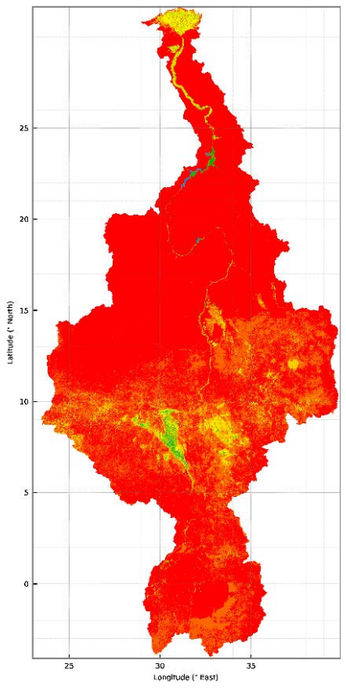

ET Incremental [mm/year]

- 0
- 0 - 500
- 500 - 1000
- 1000 - 1500
- 1500 - 2000
- 2000 - 2500
- 2500 - 3000
- > 3000

Annex 7 Annual estimated Rainfall ET (ET_{rain}) of individual years

2010

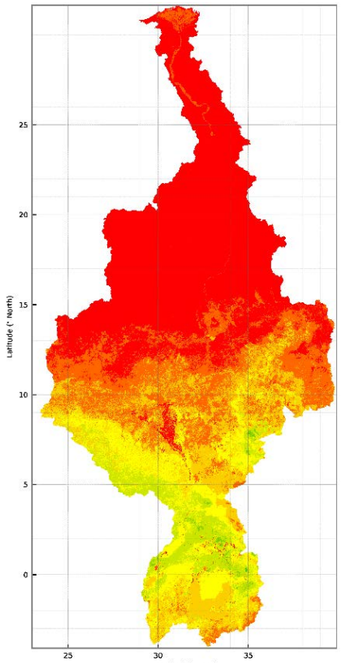

2011

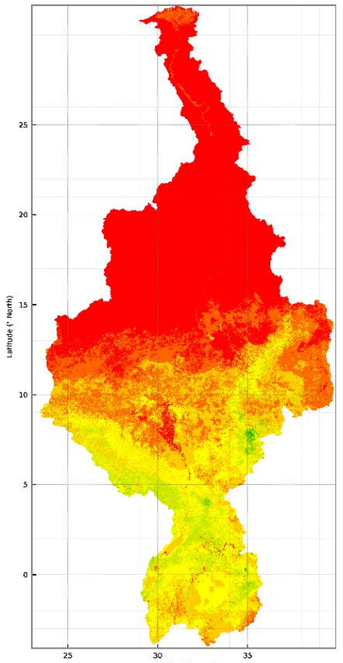

2012

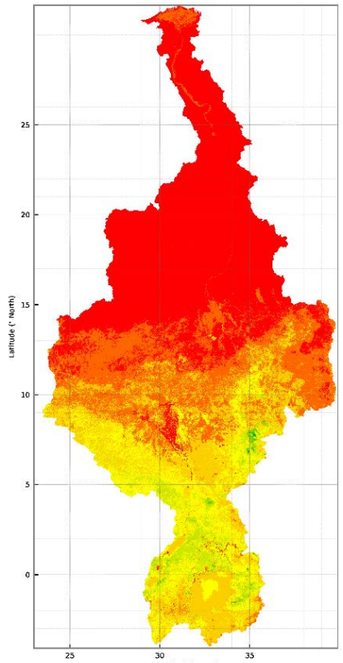

2013

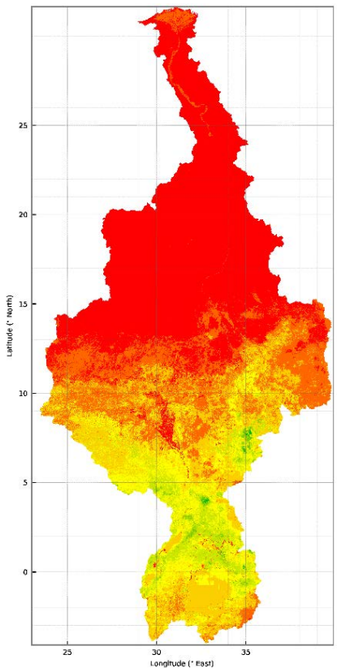

2014

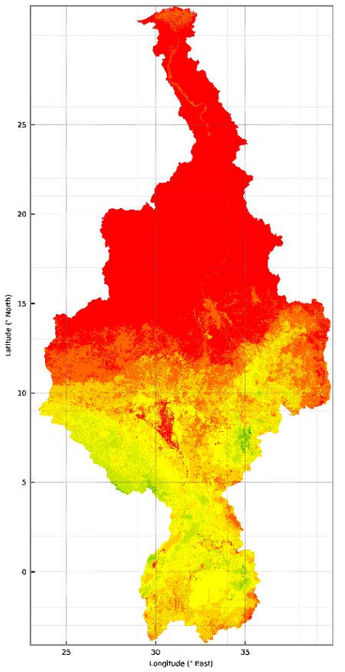

ET Rainfall [mm/year]

- 0
- 0 - 500
- 500 - 1000
- 1000 - 1500
- 1500 - 2000
- 2000 - 2500
- 2500 - 3000
- > 3000

2015

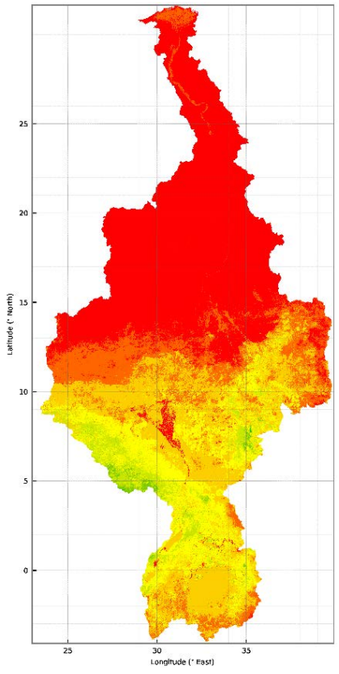

2016

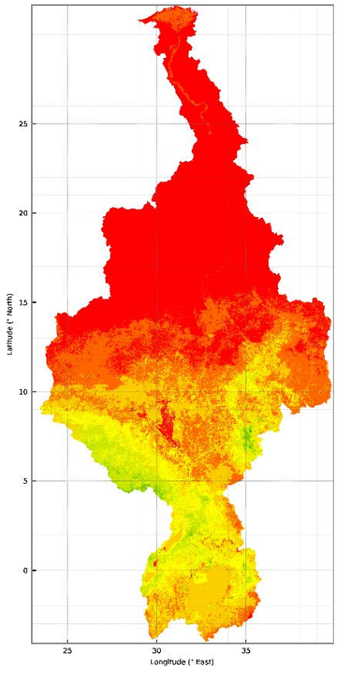

2017

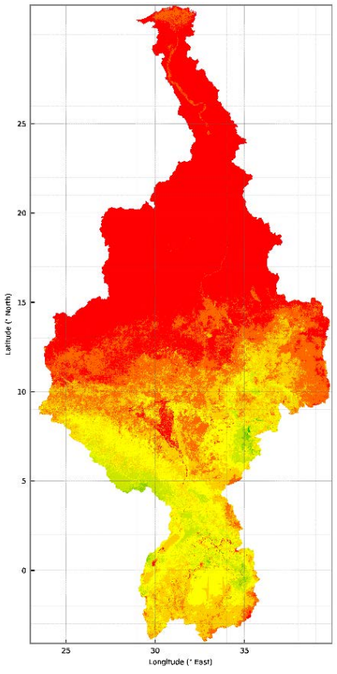

2018

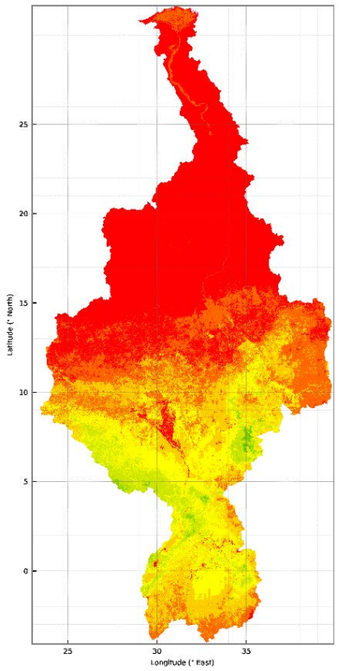

ET Rainfall [mm/year]

- 0
- 0 - 500
- 500 - 1000
- 1000 - 1500
- 1500 - 2000
- 2000 - 2500
- 2500 - 3000
- > 3000

Annex 8 Annual Water Accounting+ Sheet 1

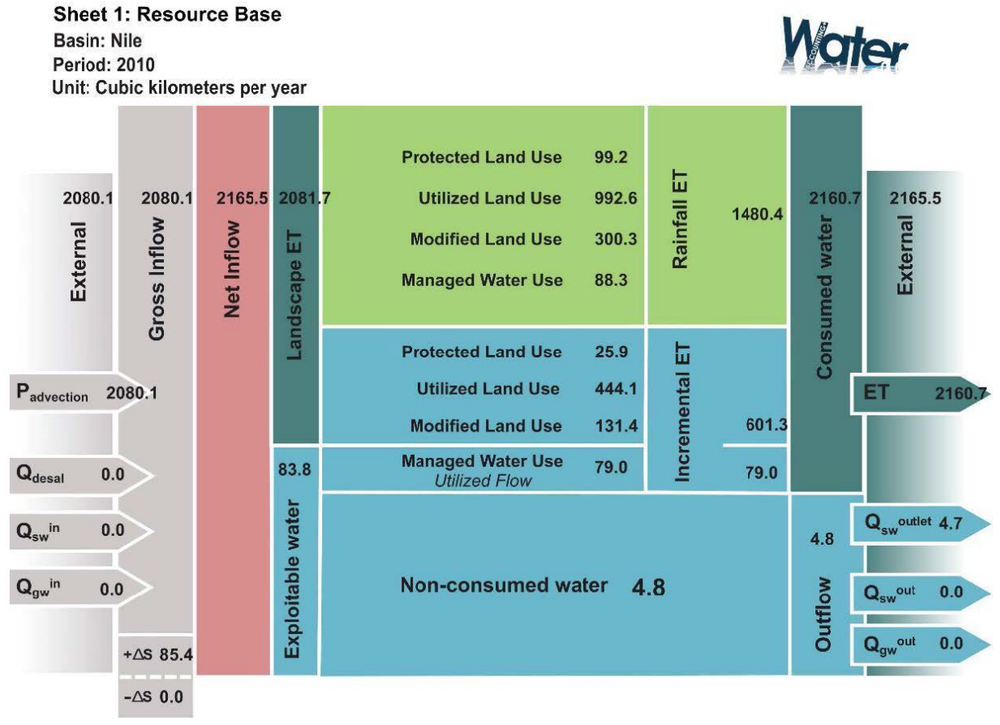

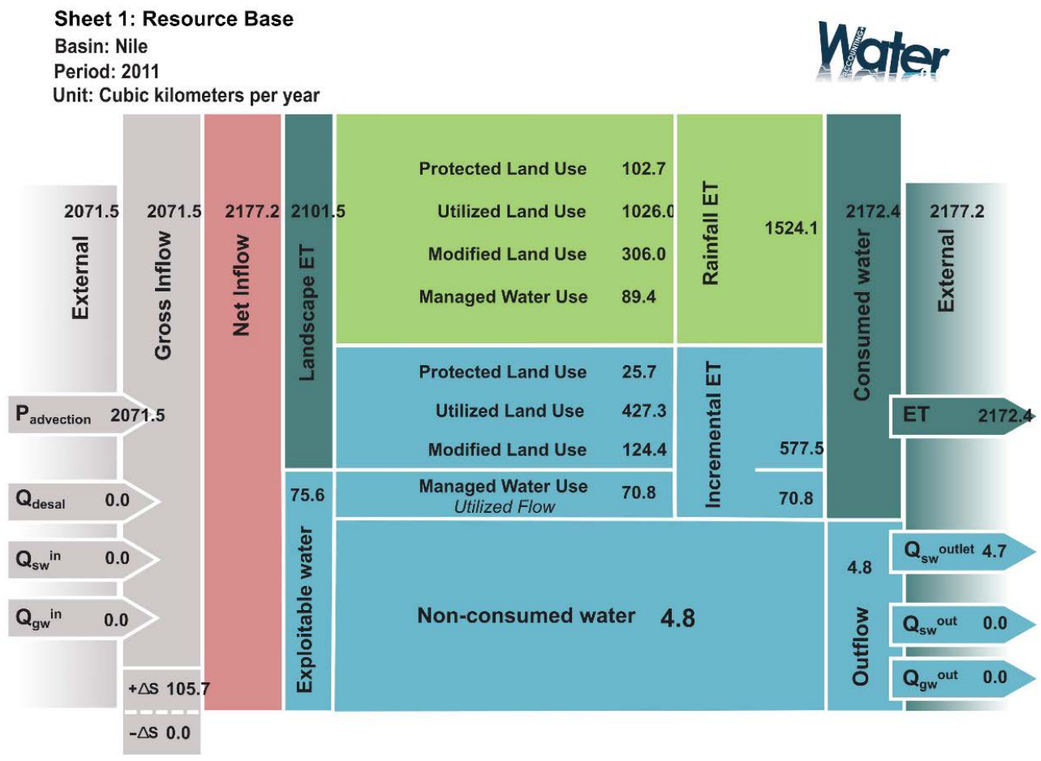

Sheet 1: Resource Base
Basin: Nile
Period: 2012
Unit: Cubic kilometers per year

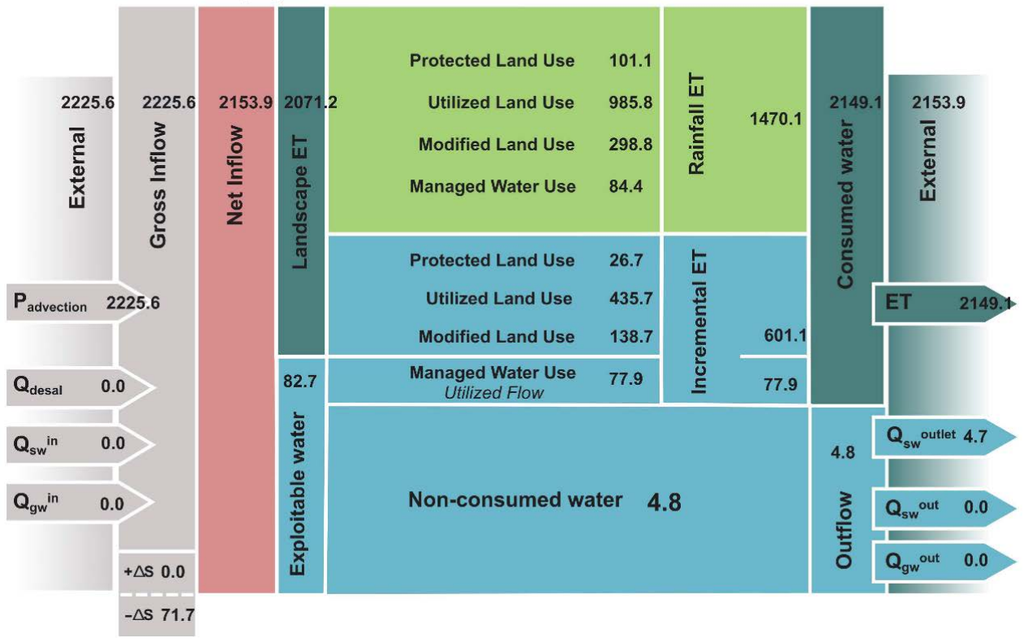

Sheet 1: Resource Base
Basin: Nile
Period: 2013
Unit: Cubic kilometers per year

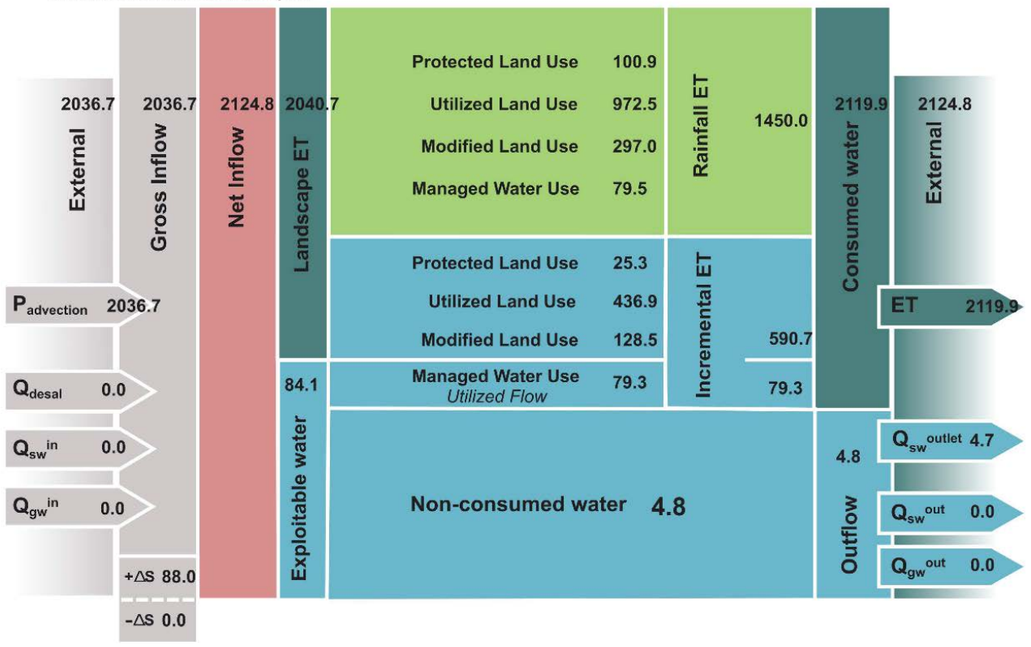

Sheet 1: Resource Base
Basin: Nile
Period: 2014
Unit: Cubic kilometers per year

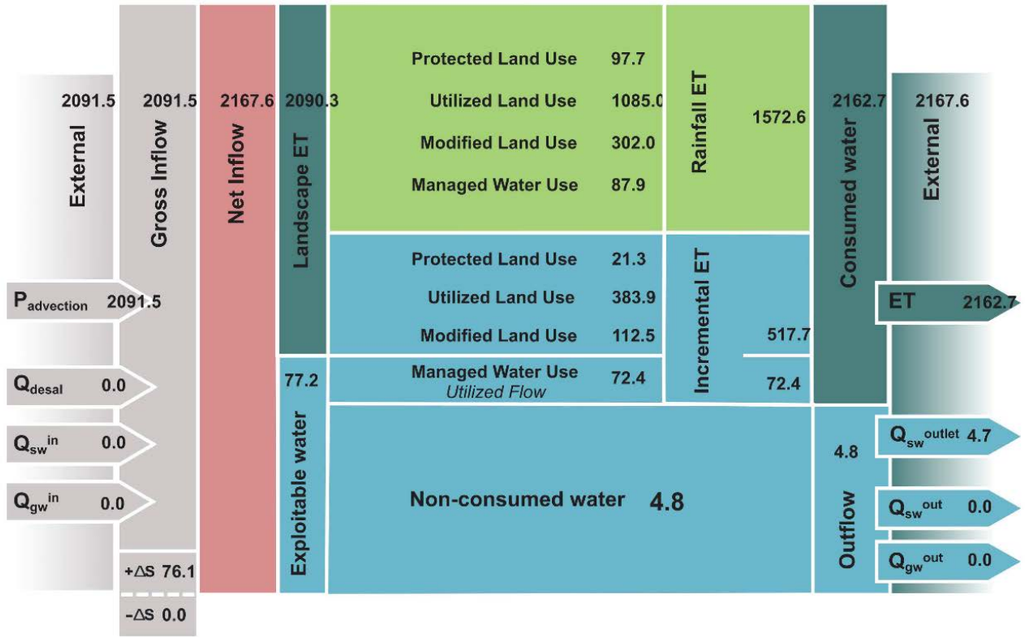

Sheet 1: Resource Base
Basin: Nile
Period: 2015
Unit: Cubic kilometers per year

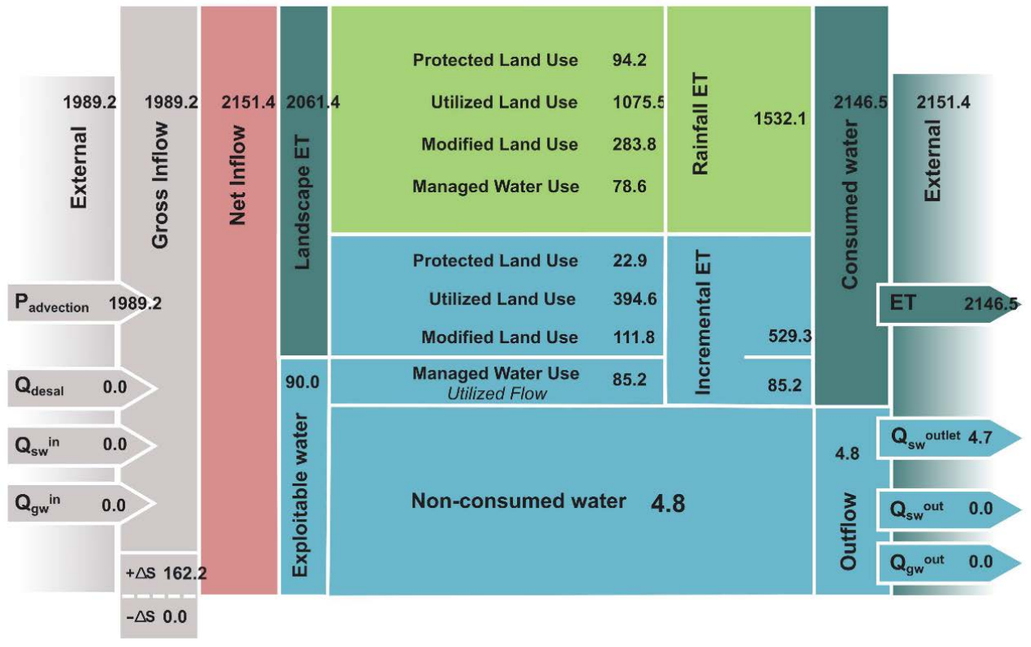

Sheet 1: Resource Base
Basin: Nile
Period: 2016
Unit: Cubic kilometers per year

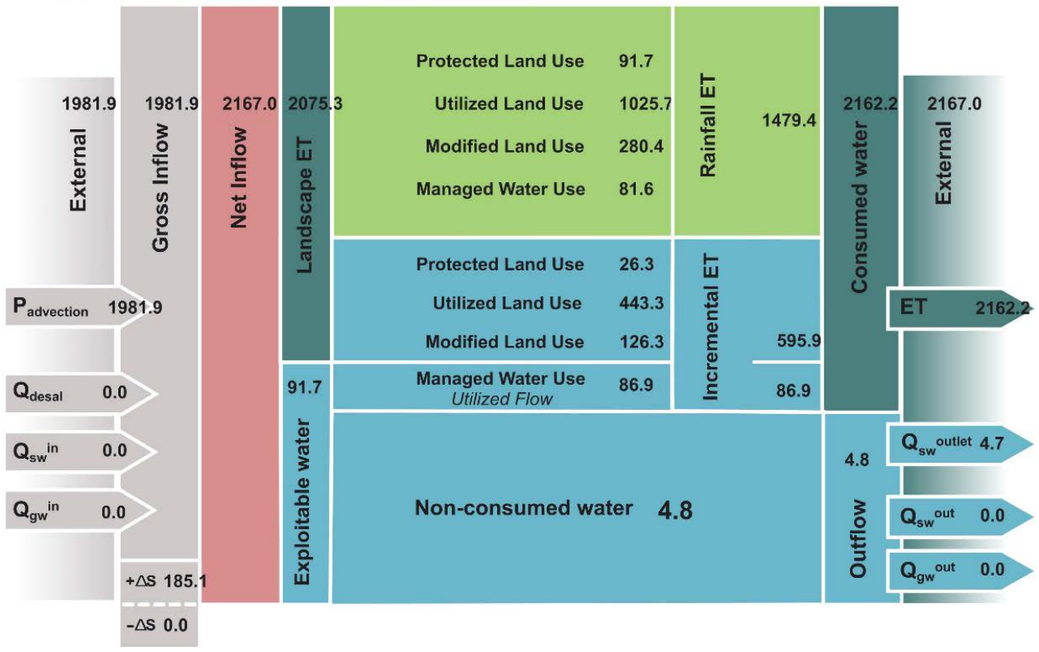

Sheet 1: Resource Base
Basin: Nile
Period: 2017
Unit: Cubic kilometers per year

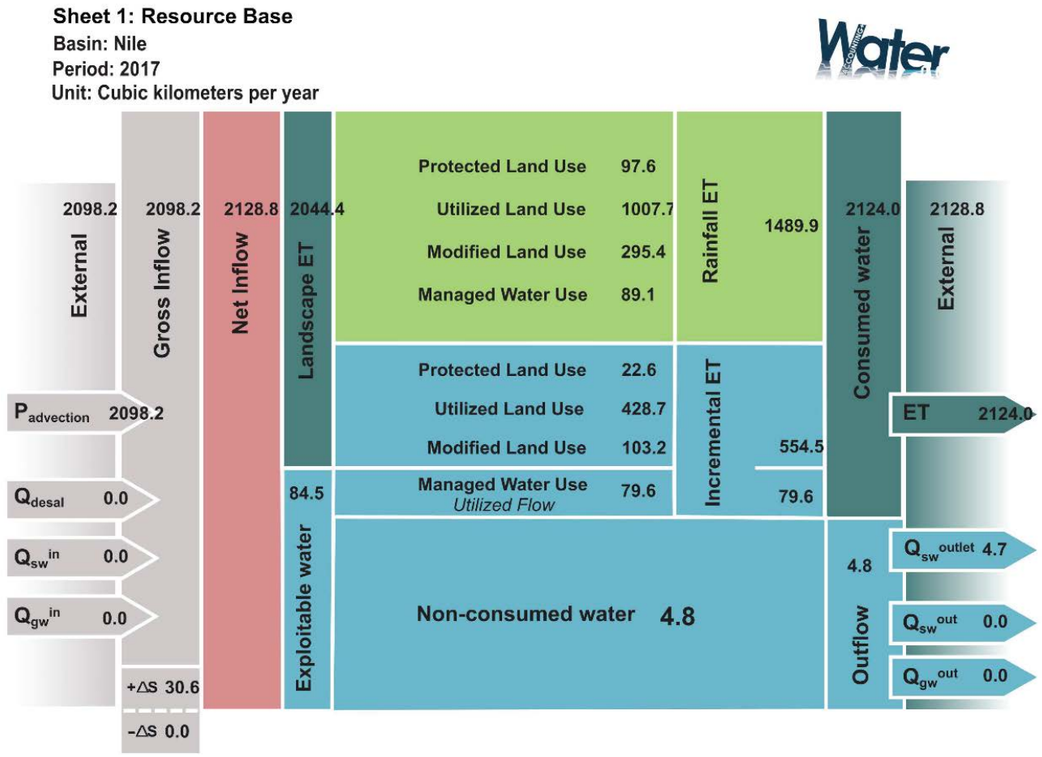

Sheet 1: Resource Base
Basin: Nile
Period: 2018
Unit: Cubic kilometers per year

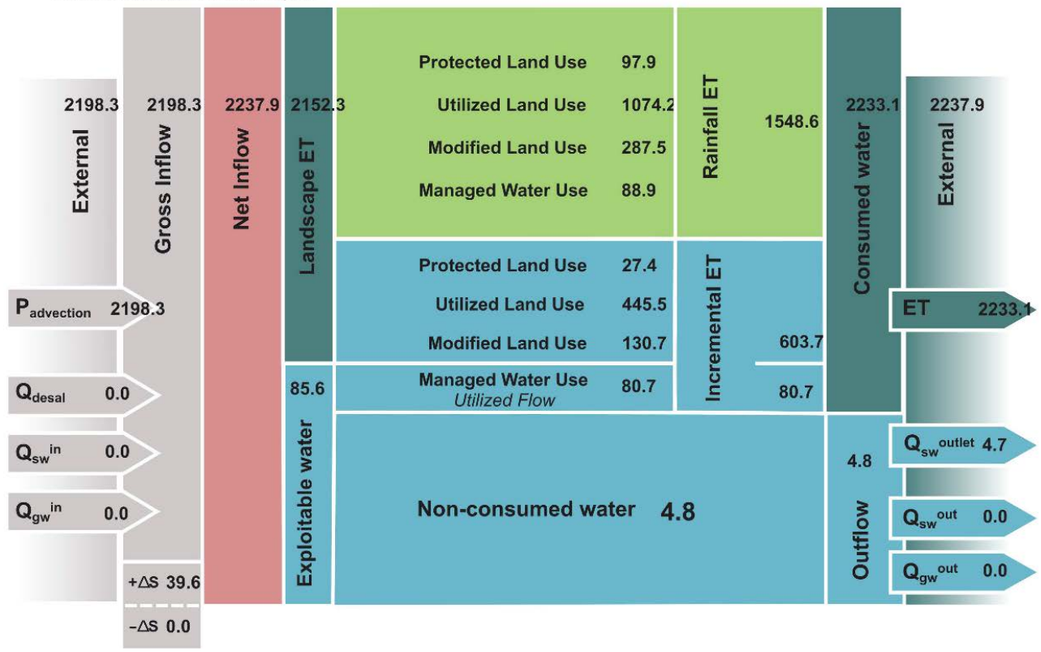

Water Accounting in the Nile River Basin

This report describes the water accounting study for the Nile River Basin carried out by IHE-Delft using the Water Productivity (WaPOR) data portal of the Food and Agricultural Organization (FAO).

The Nile River Basin faces a huge challenge in terms of water security. With an expected doubling of the population in the basin in the next twenty five years, water supply in the basin will be further depleted as demands for agriculture, domestic and industry continues to grow. Water availability in the basin will also be threatened by climate change and variability and pollution from increased agricultural and industrial activities and from urban areas. However with limited up-to-date ground observations, in terms of duration, completeness and quality of the hydro-meteorological records it is difficult to draw an appropriate picture of the water resources conditions. The Water Accounting Plus (WA+) system designed by IHE Delft with its partners FAO and IWMI has been applied to gain full insights into the state of the water resources in the basin.

Funded by:

Ministry of Foreign Affairs of the Netherlands

Frame consortium:

eleaf FEED THE WORLD

ITC

vito vision on technology

UNIVERSITY OF TWENTE.

WATERWATCH FOUNDATION

ISBN 978-92-5-132982-5

9 789251 329825

CA9895EN/1/07.20